Composite model for DNA torsion dynamics

Mariano Cadoni* and Roberto De Leo†
Dipartimento di Fisica, Università di Cagliari and INFN, Sezione di Cagliari, Cittadella Universitaria, 09042 Monserrato, Italy

Giuseppe Gaeta‡
Dipartimento di Matematica, Università di Milano, via Saldini 50, I-20133 Milano, Italy

(Received 21 April 2006; published 28 February 2007)

DNA torsion dynamics is essential in the transcription process; a simple model for it, in reasonable agreement with experimental observations, has been proposed by Yakushevich (Y) and developed by several authors; in this, the nucleotides (the DNA subunits made of a sugar-phosphate group and the attached nitrogen base) are described by a single degree of freedom. In this paper we propose and investigate, both analytically and numerically, a "composite" version of the Y model, in which the sugar-phosphate group and the base are described by separate degrees of freedom. The model proposed here contains as a particular case the Y model and shares with it many features and results, but represents an improvement from both the conceptual and the phenomenological point of view. It provides a more realistic description of DNA and possibly a justification for the use of models which consider the DNA chain as uniform. It shows that the existence of solitons is a generic feature of the underlying nonlinear dynamics and is to a large extent independent of the detailed modeling of DNA. The model we consider supports solitonic solutions, qualitatively and quantitatively very similar to the Y solitons, in a fully realistic range of all the physical parameters characterizing the DNA.

DOI: 10.1103/PhysRevE.75.021919 PACS number(s): 87.15.Aa, 05.45.Yv

I. INTRODUCTION

The possibility that nonlinear excitations—in particular, kink solitons or breathers—in DNA chains play a functional role has attracted the attention of biophysicists as well as nonlinear scientists since the pioneering paper of Englander *et al.* [1], and the works by Davydov on solitons in biological systems [2].

A number of mechanical models of the DNA double chain [3] have been proposed over the years, focusing on different aspects of the DNA molecule and on different biological, physical, and chemical processes in which DNA is involved. A discussions of such attempts is given in the book by Yakushevich [4] and in the review paper by Peyrard [5] (see also the conference [6]).

The structure and functioning of DNA are described, e.g., in [7–9]. See also [6,10] for the role of nonlinear dynamics modeling in the understanding of DNA, and [11–13] for DNA single-molecule experiments [14].

In recent years, two models have been extensively studied in the nonlinear physics literature; these are the model by Peyrard and Bishop [15] (and the extensions of this formulated by Dauxois [16] and later on by Barbi, Cocco, Peyrard, and Ruffo [17,18]; see also Cocco and Monasson [19]. More recent advances are discussed in [5,20–23]) and the one by Yakushevich [24]; we will refer to these as the PB and the Y models, respectively.

Original versions of these models are discussed in [25]; they are put in perspective within a "hierarchy" of DNA models in [26]. An attempt to blend together the two is given in [27]; see also [28]. Interplay between radial and torsional degrees of freedom is considered more organically in [17,18].

The PB model is primarily concerned with DNA denaturation, and describes degrees of freedom related to "straight" (or "radial") separation of the two helices which are wound together in the DNA double helical molecule. On the other hand, the Y model—on which we focus in this paper—is primarily concerned with rotational and torsional degrees of freedom of the DNA molecule, which play a central role in the process of DNA transcription [29].

In this model, one studies a system of nonlinear equations which in the continuum limit reduce to a pair of sine-Gordon type equations; the relevant nonlinear excitations are kink solitons—which are solitons in both the dynamical and topological sense—which describe the unwinding of the double helix in a "bubble" of about 20 bases.

The main interests of the model lies in the identification of this unwound bubble with the transcription region [30]. The proposal of Englander *et al.* [1] was that if the nonlinear excitations are not created or forced by the RNA polymerase (RNAP) but are anyway present due to the nonlinear dynamics of the DNA double helix itself, a number of questions—in particular, concerning energy flows—receive a simple explanation. Thus their model, and subsequent ones continuing their research, are not concerned with the DNA-RNAP complex, but the dynamics of the DNA double helix alone.

The Y model has been studied in a number of papers, in particular for what concerns its solitonic solutions; see in particular [26,27,31–34]. It has been shown that it gives a correct prediction of quantities related to small amplitude dynamics, such as the frequency of small torsional oscillations; and also of quantities related to fully nonlinear dynamics, such as the size of solitonic excitations describing transcription bubbles [4,25]. Moreover, in its "helicoidal"

*Electronic address: mariano.cadoni@ca.infn.it
†Electronic address: roberto.deleo@ca.infn.it
‡Electronic address: gaeta@mat.unimi.it

version, it provides a scenario for the formation of nonlinear excitation out of linear normal modes lying at the bottom of the dispersion relation branches [25]. On the other hand, it is not capable of providing a satisfactory prediction for other quantities: in particular, if we try to fit the observed speed of transversal waves along the chain [4], this is possible only upon assuming unphysical values for the coupling constants [26].

The Y model is also a very simple one, and adopts very strong simplifying assumptions (of the same kind as in the PB model). In particular, two quite strong features of the models are that: (a) there is a single (angular) degree of freedom for each nucleotide; and (b) all bases are considered as identical.

These are in a sense at the basis of the success of the model, in that thanks to these features the model can be solved exactly and one can check that predictions allowed by the model correspond to the real world situations for certain specific quantities. But the features mentioned above are of course not in agreement with the real situation.

Indeed, it is well-known that bases are quite different from each other, and in particular purines are much bigger than pirimidines; hence feature (b)—albeit necessary for an analytical treatment of the model—is definitely unrealistic. Moreover, it is quite justified to consider several groups of atoms within a single nucleotide (the phosphodiester chain, the sugar ring, and the nitrogen base) as substantially different subunits; but these—in particular, the sugar ring—have some degree of flexibility, and what is more they have a considerable freedom of displacement—in particular, for what concerns torsional and rotational movements—with respect to each other. Thus, even in a simple modeling, feature (a) is not justified *per se*, and it seems quite appropriate to consider several subunits within each nucleotide. In this sense, we will speak of a *composite Yakushevich* (*Y*) *model* [35].

In this work we propose and study a composite Y model (in the sense mentioned above), in which we describe the state of each nucleotide by *two* independent angular degrees of freedom, one related to the sugar-phosphate group and one to the nitrogen base.

It will turn out that the Y model, which can be considered as a particular case of our model, captures to a large extent (this will be made more precise in the following) the essential features of DNA nonlinear dynamics.

On the other hand, the more realistic geometry of the composed model enables a drastic improvement of the descriptive power of the model at both the conceptual and the phenomenological level: the composite Y model keeps almost all the relevant features of the Y model, but it allows for a more realistic choice of the physical parameters.

The different degrees of freedom we use will play a fundamentally different role in the description of DNA nonlinear dynamics. The backbone degrees of freedom are "topological" and play to some extent a more relevant role, in that the solitons are mainly associated to them; while those associated to the base are "nontopological" and represent small oscillations. These different roles are specially clear when we consider the limit in which our model reduces to the standard Y model (see Sec. VIII), in which only the topological degrees of freedom are present.

This opens an interesting possibility—which we will discuss elsewhere—i.e., to consider more realistic models, in which differences among bases are properly considered, as perturbations of our idealized uniform model. As the essential features of the fully nonlinear dynamics are related only to backbone degrees of freedom, such a perturbation—albeit with a relevant difference in the quantitative values of some parameters entering in the model (the base dynamical and geometrical parameters)—should show the same kind of nonlinear dynamics as our uniform model studied here.

Finally, it should be mentioned that the model studied here disregards nonconservative effects in DNA dynamics; these are known to be relevant, as DNA is actually an overdamped system subject to random forces arising from interactions with its environment; however, in our opinion an understanding of DNA dynamics *per se* should be reached before attempting to model also its rather complex interactions with the environment.

The paper is organized as follows. In Sec. II we will briefly review some basic facts about the DNA structure and modeling. In Secs. III and IV we will set up our model, describe the interaction, and write down the equations of motions that govern its dynamics. The physical parameters characterizing our model are discussed in Sec. V. In Sec. VI we discuss the linear approximation of our dynamical system, in particular its dispersion relations. In Sec. VII we will set up the framework for the investigation of the nonlinear dynamics and the topological excitations of our model. In Sec. VIII, we will show how the Y model and Y solitons emerge as a particular case of our composite Y model and its solitons. In Sec. IX we investigate and derive numerically the solitonic solutions of our model. Finally in Sec. X we summarize our work and present our conclusions. We also give an Appendix where we write down some explicit expressions which we felt were not appropriate for inclusion in the main text but could be of interest to the specialized reader.

II. DNA STRUCTURE AND MODELING

In this section we recall some basic facts about DNA structure, directly relevant to the model to be considered, and the interactions considered by our model; see [7–9] for more details on DNA structure and behavior.

We will refer for definiteness to the standard conformation of the molecule (B-DNA); in this the pitch of the helix corresponds to ten base pairs, and the distance (measured along the axis of the helix) between successive base pairs is $\delta = 3.4$ Å.

DNA is a gigantic polymer, made of two helices wound together. The general structure of each helix can be described as follows (see also Fig. 1). The helix is made of a sugar-phosphate backbone, to which bases are attached. The backbone has a regular structure consisting of repeated identical units (sugar-phosphate groups, also called *backbone units* in the following), consisting of a segment of the phosphodiester chain and a sugar ring (two carbon atoms being part of both the chain and the ring); bases are attached to a specific site on the sugar ring and are of four possible types. These are

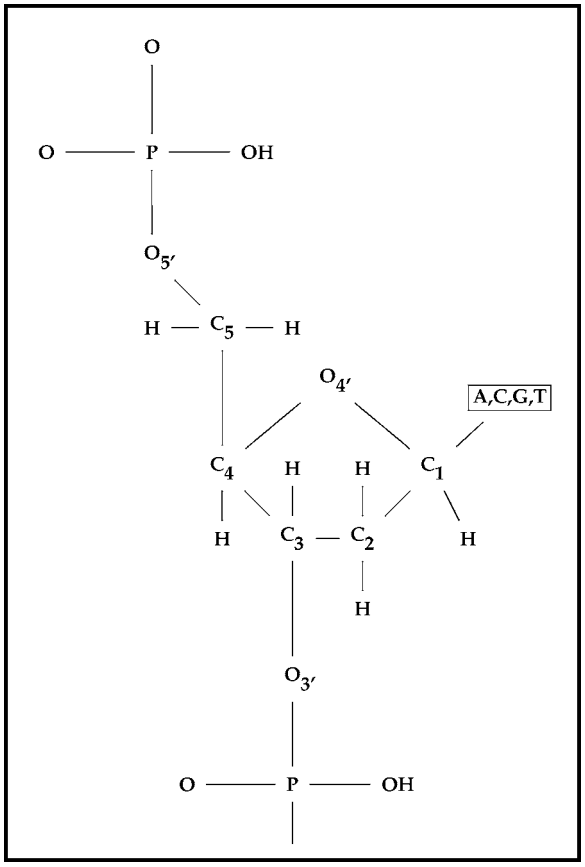

FIG. 1. The structure of a DNA helix. The figure shows a nucleotide and the PO_4 group in the next one, to emphasize the periodicity of the sequence; nitrogen bases are attached to the C_1 atom in the sugar ring.

either purines, i.e., adenine (A) or guanine (G), or pyrimidines, i.e., cytosine (C) or thymine (T). It should be noted that the bases are rather rigid structures, and have an essentially planar configuration. A unit of each helix, i.e., the complex of a backbone unit and the attached base, is called a *nucleotide*.

The structure of the double helix makes that to each base on the one helix corresponds a base on the other helix, hence we have base pairs. Each base has only a possible partner in a base pair, the (Watson-Crick) base pairs being A-T and G-C. Bases in a pair are linked together via hydrogen bonds (two for A-T pairs, three for G-C pairs). The base pairs can be "opened" quite easily, the dissociation energy for each H-bond being of the order of 0.04 eV, hence $\Delta E \simeq 0.1 \pm 0.02$ eV per base pair. Opening is instrumental to a number of processes undergone by DNA, among which notably transcription, denaturation, and replication.

The atoms on each helix are of course held together by covalent bonds; apart from these, other interactions should be taken into account when attempting a description of the DNA molecule.

(1) The backbone structure has some rigidity; in particular, it would resist movements which represent a torsion of one backbone unit with respect to neighboring ones. We will refer to the interaction responsible for the forces resisting these torsions as *torsional interactions*.

(2) As already mentioned, the two bases composing a base pair are linked together by hydrogen bonds; we will refer to the interaction mediated by these as *pairing interactions*.

(3) Each base interacts with neighboring bases on the same chain via electrostatic forces (bases are strongly polar); these make energetically favorable the conformation in which bases are regularly stacked on top of each other, and therefore are referred to as *stacking interaction*.

(4) Finally, water filaments—thus, essentially, bridges of hydrogen bonds—link units at different sites (these are also known as Bernal-Fowler filaments [2]). In particular, they have a good probability to form between nucleotides which are a half-turn of the helix apart on different chains, i.e., which are near to each other in space due to the double helix geometry; these water filaments-mediated interactions are therefore also called *helicoidal interactions* [36]. We stress that these are quite weaker than other interactions, and can be safely overlooked when we consider the fully nonlinear regime. They are instead of special interest when discussing small amplitude (low energy) dynamics, as they remove a degeneration and moreover—just because of their weakness—are easily excited and introduce a length scale in the dispersion relations (see below).

If we consider deviations from the equilibrium configurations, motions will not be completely free: the molecule is densely packed in space, and the presence of the sugar-phosphate backbone—and of neighboring bases—will cause steric hindrances to the base movements. In particular, for the rotations in a plane perpendicular to the double helix axis, the bases will not be able to rotate around the C_1 atom for more than a maximum angle φ_0 without colliding with the sugar-phosphate group.

This will lead of course to complex behaviors as the DNA helix gets unwound; in particular, as φ gets near to its limit value φ_0 we expect some kind of essentially (if not mathematically) discontinuous behavior. This should not be seen as a shortcoming of the model: it is indeed well-known that bases rotate in a complex way while flipping about the DNA axis (see, e.g., [37]).

Finally, we mention that here we consider a DNA molecule without taking into account its macroconformational features; that is, we consider an "ideal" molecule, disregarding supercoiling, organization in histones, and all that [7].

III. COMPOSITE Y MODEL

As mentioned above, we will model the molecule as made of different parts (units), each of them behaving as a single element, i.e., as a rigid body. We consider each sugar-phosphate group $\mathcal{N}$, i.e., segment of the phosphodiester chain together with a sugar, as a unit (backbone unit), to which a base $\mathcal{B}$ (considered again as a single unit) is attached.

We will model each of the helices in the DNA double chain as an array of elements (nucleotides) made of two subunits; one of these subunits models the sugar-phosphate group $\mathcal{N}$, the other the nitrogen base $\mathcal{B}$. We will consider the bases as all equal, thus disregarding the substantial difference between them [38]. The chains—and thus the arrays—will be considered as infinite.

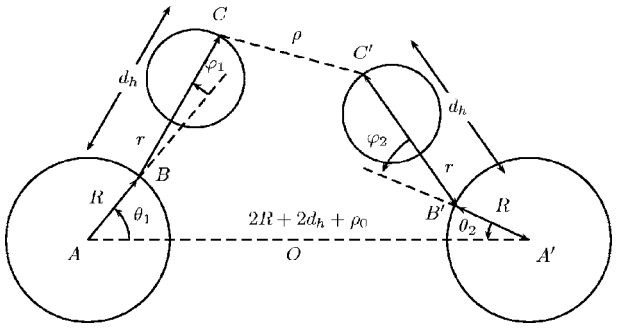

FIG. 2. A base pair in our model. The origin of the coordinate system is O. The angles θ_1 between the lines AO and AB and θ_2 between $A'O$ and $A'B'$ correspond to torsion of sugar-phosphate backbone with respect to the equilibrium B-DNA conformation; the angles φ_1 between the line AB and the line BC, and φ_2 between $A'B'$ and $B'C'$ correspond to rotation of bases around the C_1-N bond linking them to the nucleotide. All angles are in counterclockwise direction; thus the angles θ_2 and φ_2 in the figure are negative. Points B and B' correspond to p_c in the main text; points C and C' correspond to p_h in the main text.

We will use a superscript $a=1,2$ to distinguish elements on the two chains, and a subscript $i \in \mathbf{Z}$ to identify the site on the chains. Thus at site i on chain a we will have the backbone unit $\mathcal{N}_i^{(a)}$ and the base $\mathcal{B}_i^{(a)}$. The base pairing will be between bases $\mathcal{B}_i^{(1)}$ and $\mathcal{B}_i^{(2)}$, while stacking interaction will pair base $\mathcal{B}_i^{(a)}$ to bases $\mathcal{B}_{i+1}^{(a)}$ and $\mathcal{B}_{i-1}^{(a)}$.

We will consider each backbone unit $\mathcal{N}_i^{(a)}$ as a disk; bases will be seen as disks themselves, with a point on the border of $\mathcal{B}_i^{(a)}$ attached via an inextensible rod (modeling the bond) to a point p_c on the border of $\mathcal{N}_i^{(a)}$; these points on $\mathcal{B}$ and $\mathcal{N}$ represent the locations of the N atom on $\mathcal{B}$ and of the C_1 atom on $\mathcal{N}$ involved in the chemical bond attaching the base to the sugar-phosphate group (the points p_c on the two bases in a pair are denoted, for graphical convenience, as B and B' in Fig. 2). The rod can rotate at most by an angle $\pm\varphi_0$; on the other hand, the disk $\mathcal{N}$ can rotate completely around its axis.

We also single out a point p_h on the border of the disk modeling the base; this represents the atom(s) which form the H bond with the corresponding base on the other DNA chain (the points p_h on the two bases in a pair are denoted—again for graphical convenience—as C and C' in Fig. 2). The disks (i.e., the elements of our model) are subject to different kinds of forces, corresponding to those described above: torsional forces resisting the rotation of one disk $\mathcal{N}_i^{(a)}$ with respect to neighboring disks $\mathcal{N}_{i+1}^{(a)}$ and $\mathcal{N}_{i-1}^{(a)}$ on the same chain; stacking forces between a base $\mathcal{B}_i^{(a)}$ and neighboring bases $\mathcal{B}_{i+1}^{(a)}$ and $\mathcal{B}_{i-1}^{(a)}$ on the same chain; pairing forces between bases $\mathcal{B}_i^{(1)}$ and $\mathcal{B}_i^{(2)}$ in the same base pair; and finally, helicoidal forces correspond to hydrogen bonded Bernal-Fowler filaments linking bases $\mathcal{B}_i^{(1)}$ and $\mathcal{B}_{i\pm5}^{(2)}$ (and $\mathcal{B}_i^{(2)}$ and $\mathcal{B}_{i\pm5}^{(1)}$).

We are primarily interested in the torsional dynamics. Thus for each element we will consider torsional movements, hence a rotation angle (with respect to the equilibrium conformation); these will be denoted as $\theta_i^{(a)}$ for the backbone unit $\mathcal{N}_i^{(a)}$, and $\varphi_i^{(a)}$ for the base $\mathcal{B}_i^{(a)}$. Only these rotations will be allowed in our model. All angles will be positive in counterclockwise sense.

The angles θ represent a torsion of the sugar-phosphate backbone with respect to the equilibrium configuration; thus they are related to unwinding of the double helix. On the other hand, the angles φ represent a rotation of the base with respect to the corresponding backbone unit (we stress the fact that we are considering only rotations in the plane perpendicular to the axis of the double helix); the presence of backbone atoms constrains rotation of the base and hence the range of φ [39]. Thus, as mentioned above, the angles will have a different range of values:

$$\theta_i^{(a)} \in \mathbf{R}, \quad \varphi_i^{(a)} \in [-\varphi_0, \varphi_0] \varphi_0 < \pi. \tag{3.1}$$

It should be stressed that—just on the basis of these different ranges of variations—there will be a substantial difference between the degrees of freedom described by the angles: those described by θ angles will be *topological* degrees of freedom, while those described by φ angles will only describe local and (relatively) small motions—hence φ describe nontopological degrees of freedom.

IV. THE LAGRANGIAN

We will now translate the above discussion into a Lagrangian defining our model. This will be written as

$$L = T - (U_t + U_s + U_p + U_h), \tag{4.1}$$

where T is the kinetic energy, and U_a are the potential energies for the different interactions listed above, i.e., U_t is the backbone torsional potential; U_s is the stacking potential; U_p is the pairing potential; and U_h is the helicoidal potential.

These interactions will be modeled by two-body potentials, for which we use the notation V_a, to be summed over all interacting pairs in order to produce the U_a.

We denote by I the moment of inertia (around center of mass) of disks modeling the backbone units, and by I_B the moment of inertia of bases around the C_1 atom in the sugar ring; as the bases cannot rotate around their center of mass, $I_B = mr^2$ where m is the base mass and r is the distance between the C_1 atom in the sugar and the center of mass of the base.

A. Kinetic energy

In computing the kinetic energy, it will be convenient to consider Cartesian coordinates. With reference to Fig. 2, the Cartesian coordinates in the (x,y) plane orthogonal to the double helix axis of relevant points will be as follows.

The center of disks, representing the position of the phosphodiester chain, will be $(x_o^{(a)}, y_o^{(a)})$; the point on the border of the disks representing the C_1 atom to which the base disks are attached will be $(x_c^{(a)}, y_c^{(a)})$. The center of mass of the bases will be $(x_b^{(a)}, y_b^{(a)})$, and the point on the border of the disks modeling bases representing the atom(s) forming the H bonds will be $(x_h^{(a)}, y_h^{(a)})$.

In terms of the $\{\theta, \varphi\}$ angles, these are given by (we omit the site index i for ease of writing, and give condensed formulas for the two chains, with first sign referring to chain 1):

$$x_o^{(1,2)} = \mp a, \quad y_o^{(1,2)} = 0;$$

$$x_c^{(1,2)} = x_o^{(1,2)} \pm R\cos(\theta^{(1,2)}), \quad y_c^{(1,2)} = \pm R\sin(\theta^{(1,2)});$$

$$x_b^{(1,2)} = x_c^{(1,2)} \pm r\cos(\theta^{(1,2)} + \varphi^{(1,2)}),$$

$$y_b^{(1,2)} = y_c^{(1,2)} \pm r\sin(\theta^{(1,2)} + \varphi^{(1,2)});$$

$$x_h^{(1,2)} = x_c^{(1,2)} \pm d_h\cos(\theta^{(1,2)} + \varphi^{(1,2)}), \tag{4.2}$$

$$y_h^{(1,2)} = y_c^{(1,2)} \pm d_h\sin(\theta^{(1,2)} + \varphi^{(1,2)}).$$

Here and in the following we denote by R the radius of disks describing backbone units, i.e., the length of the segments AB and $A'B'$ in Fig. 2 (this is the distance from the phosphodiester chain to the C_1 atom); and by r the distance between the center of mass of bases and the border of the disk modeling the backbone unit (i.e., the C_1 atom). We also denote by d_h the lengths (supposed equal) of the segments BC and $B'C'$ joining the C_1 atom on the sugar-phosphate group and the atoms of the bases forming the hydrogen bond linking this to the complementary base. The parameter a corresponds to the distance between the double helix axis and the phosphodiester chain, whereas ρ_0 is the distance between points C and C' in the equilibrium configuration. The previous parameters are obviously related by the equation $2a = 2R + 2d_h + \rho_0$.

With this notation, and standard computations, the kinetic energy of each nucleotide is written as

$$T_i^{(a)} = \frac{1}{2}\{mr^2\dot{\varphi}^2 + 2mr(r + R\cos\varphi)\dot{\theta}\dot{\varphi} + [I + m_B(R^2 + r^2) + 2mRr\cos\varphi]\dot{\theta}^2\},$$

where we have suppressed super- and subscripts for ease of reading. Thus the total kinetic energy for the double chain is

$$T = \sum_a \sum_i T_i^{(a)} = \frac{1}{2}\sum_a \sum_i [mr^2(\dot{\varphi}_i^{(a)})^2 + 2mr[r + R\cos(\varphi_i^{(a)})]\dot{\theta}_i^{(a)}\dot{\varphi}_i^{(a)} + (I + m_B(R^2 + r^2) + 2mRr\cos(\varphi_i^{(a)}))(\dot{\theta}_i^{(a)})^2]. \tag{4.3}$$

B. Potential terms

So far we have actually considered a general class of composite Y models, in that we have not specified the interaction potentials, which are needed to have a definite model.

We have now to specify our model by fixing analytical expressions for the potentials in Eq. (4.1). As one of our aims is to compare the results obtained by a composite Y model with those obtained with the simple Y model, we will make choices with the same physical content as those made by Yakushevich.

1. Torsional interactions

Torsional forces will depend only on difference of angles (measured with respect to the equilibrium configuration) of neighboring units on the same phosphodiester chain; thus

$$U_t = \sum_a \sum_i V_t(\theta_{i+1}^{(a)} - \theta_i^{(a)}). \tag{4.4}$$

The potential V_t must have a minimum in zero and be 2π-periodic in order to take into account the fundamentally discrete and quantum nature of the phosphodiester chain. Here we will take the simplest such function [40], i.e., (adding an inessential constant so that the minimum corresponds to zero energy),

$$V_t[x] = K_t[1 - \cos(x)], \tag{4.5}$$

where K_t is a dimensional constant. Thus our choice for torsional interactions will be

$$U_t = K_t\sum_a \sum_i [1 - \cos(\theta_{i+1}^{(a)} - \theta_i^{(a)})]. \tag{4.6}$$

The harmonic approximation for this is of course

$$U_t^q = \frac{1}{2}K_t\sum_a \sum_i (\theta_{i+1}^{(a)} - \theta_i^{(a)})^2.$$

2. Stacking interactions

Stacking between bases will only depend on the relative displacement of neighboring bases on the same helix in the plane orthogonal to the double helix axis [41]. That is, we have

$$U_s = \sum_a \sum_i V_s(\sigma_i^{(a)}), \tag{4.7}$$

where

$$\sigma_i^{(a)} := \sqrt{(x_{i+1}^{(a)} - x_i^{(a)})^2 + (y_{i+1}^{(a)} - y_i^{(a)})^2}, \tag{4.8}$$

where $x_i^{(a)}$, $y_i^{(a)}$ are the coordinates of the center of mass of the bases. The simplest choice corresponds to a harmonic potential [42], $V_s = (1/2)K_s\sigma^2$. This will be our choice, which again corresponds to the one made in the PB and in the Y models, so that

$$U_s = \sum_a \sum_i \frac{K_s}{2}(\sigma_i^{(a)})^2. \tag{4.9}$$

We should, however, express this in terms of the θ and φ angles. With standard algebra, using Eq. (4.2), we obtain

$$U_s = \frac{1}{2}K_s\sum_a \sum_i 2[R^2 + r^2 - R^2\cos(\theta_{i+1}^{(a)} - \theta_i^{(a)}) - r^2\cos[(\theta_{i+1}^{(a)} - \theta_i^{(a)}) + (\varphi_{i+1}^{(a)} - \varphi_i^{(a)})] - Rr(\cos[(\theta_{i+1}^{(a)} - \theta_i^{(a)}) + \varphi_{i+1}^{(a)}] + \cos[(\theta_{i+1}^{(a)} - \theta_i^{(a)}) - \varphi_i^{(a)}]) + Rr(\cos(\varphi_{i+1}^{(a)}) + \cos(\varphi_i^{(a)}))]. \tag{4.10}$$

3. Pairing interactions

Pairing interactions are due to stretching of the hydrogen bonds linking bases in a pair. Introducing a paring potential V_p which models the H bonds, we have

$$U_p = \sum_i V_p(\theta_i^{(1)}, \theta_i^{(2)}, \varphi_i^{(1)}, \varphi_i^{(2)}). \tag{4.11}$$

We note that H bonds are strongly directional, so that they are quickly disrupted once the alignment between pairing bases is even partially lost. This feature is traditionally disregarded in the Y model, where it is assumed that V_p only depends on the distance

$$\rho_i := \sqrt{(x_i^{(1)} - x_i^{(2)})^2 + (y_i^{(1)} - y_i^{(2)})^2} \tag{4.12}$$

between the interacting bases [43]; that is,

$$U_p = \sum_i V_p(\rho_i). \tag{4.13}$$

As for the potential V_p, there are two simple choices for this appearing in the literature. On the one hand, Yakushevich [24] suggests to consider a potential harmonic in the intrapair distance ρ (this would appear nonlinear when expressed through rotation angles) and this has been kept in subsequent discussions and extensions of her model [4]. On the other hand, Peyrard and Bishop [15] consider a Morse potential; again this has been kept in subsequent discussions and extensions of their model [5].

There is no doubt that the Morse potential is more justified in physical terms; however, as we wish to compare our results with those of the original Y model, we will at first consider a harmonic potential

$$V_p^{(Y)}(\rho) = \frac{1}{2} K_p (\rho - \rho_0)^2, \tag{4.14}$$

where ρ_0 is the intrapair distance in the equilibrium configuration. Moreover, again in order to compare our results with those of the original Y model, we will later on set $\rho_0 = 0$. This corresponds to setting $a = R + d_h$.

These approximations can appear very crude, but experience gained (actually as preliminary work for the present investigation) with the standard Yakushevich model [44,45] suggests they do not have a great impact at the level of fully nonlinear dynamics.

We should express V_p in terms of the rotations angles. Using once again the expression (4.2), we have with standard computations that

$$\begin{aligned}\rho_i^2 := (x_i^{(1)} - x_i^{(2)})^2 + (y_i^{(1)} - y_i^{(2)})^2 = 2[&2a^2 + R^2 + d_h^2 \\ &+ R^2 \cos(\theta_i^{(1)} - \theta_i^{(2)}) + d_h^2 \cos[(\theta_i^{(1)} - \theta_i^{(2)}) + (\varphi_i^{(1)} - \varphi_i^{(2)})] \\ &+ R d_h (\cos\varphi_i^{(1)} + \cos\varphi_i^{(2)} + \cos[(\theta_i^{(1)} - \theta_i^{(2)}) + \varphi_i^{(1)}] \\ &+ \cos[(\theta_i^{(1)} - \theta_i^{(2)}) - \varphi_i^{(2)}]) - 2aR(\cos(\theta_i^{(1)}) + \cos(\theta_i^{(2)})) \\ &- 2a d_h (\cos(\varphi_i^{(1)} + \theta_i^{(1)}) + \cos(\varphi_i^{(2)} + \theta_i^{(2)}))].\end{aligned} \tag{4.15}$$

With this, our choice for the pairing part of the Hamiltonian will be

$$U_p = \sum_i V_p(\rho_i). \tag{4.16}$$

4. Helicoidal interactions

As mentioned above, helicoidal interaction are mediated by water filaments (Bernal-Fowler filaments [2]) connecting different nucleotides; in particular, we will consider those being on opposite helices at half-pitch distance, as they are near enough in three-dimensional space due to the double helical geometry. As the nucleotide moves, the hydrogen bonds in these filaments—and those connecting the filaments to the nucleotides—are stretched and thus resist differential motions of the two connected nucleotides.

We will, for the sake of simplicity and also in view of the small energies involved, only consider filaments forming between backbone units; thus only the θ angles will be involved in these interactions. We have therefore, introducing a helicoidal potential V_h and recalling that the pitch of the helix corresponds to ten bases in the B-DNA equilibrium configuration we are considering,

$$U_h = \sum_i V_h(\theta_{i+5}^{(1)} - \theta_i^{(2)}) + V_h(\theta_{i+5}^{(2)} - \theta_i^{(1)}). \tag{4.17}$$

As the angles θ are involved, the potential V_h should be 2π-periodic [46].

Such water filament connections involve a large number of hydrogen bonds (around ten); hence each of them is only slightly stretched, and it makes sense to consider the angular-harmonic approximation

$$V_h(\tau) = K_h[1 - \cos(\tau)] \simeq \frac{1}{2} K_h \tau^2. \tag{4.18}$$

Our choice will therefore be

$$U_h = K_h \sum_i [2 - \cos(\theta_{i+5}^{(1)} - \theta_i^{(2)}) - \cos(\theta_{i+5}^{(2)} - \theta_i^{(1)})]. \tag{4.19}$$

C. Equations of motion

In the previous sections we have set up the model, both for the geometry and the interactions; we will now study its dynamics. We denote collectively the variables as ψ^μ, with $\psi = (\varphi^{(1)}, \varphi^{(2)}, \theta^{(1)}, \theta^{(2)})$. The dynamics of the model will be described by the Euler-Lagrange equations

$$\frac{\partial L}{\partial \psi_i^\mu} - \frac{d}{dt} \frac{\partial L}{\partial \dot{\psi}_i^\mu} = 0, \tag{4.20}$$

corresponding to the Lagrangian (4.1).

We stress again (as already mentioned in the Introduction) that the model studied here—as all models of DNA dynamics in the literature—disregards nonconservative effects in DNA dynamics. As is well-known, DNA in the living cell is embedded in a fluid environment; due to interaction with this, the DNA molecule is subject to random forces, and its motion is (over)damped. Purely mechanical models of DNA aim at reaching an understanding of DNA dynamics *per se*, which is preliminary to attempts of modeling the complex DNA/environment interactions.

The equation of motion (4.20)—shown explicitly in the Appendix, see Eq. (A1)—is far too complex to be analyzed

TABLE I. Order of magnitude for the basic geometrical parameters of the DNA. Units of measure are atomic unit for masses m, 1.67×10^{-47} Kg m^2 for the inertia momenta I, angstrom for l, d_s, and d_b, respectively, the longitudinal width of bases and their distances from the relative sugars and from the relative dual base. These values have been extracted from the sample "generic" B-DNA PDB data [49], kindly provided by the Glactone Project [50], and double checked with the data from [48], that agree within 5%. Inertia momenta of bases has been evaluated with respect to rotations about the DNA's symmetry axis passing through the sugar's C_1 atom the base is attached to; the inertia momentum of the sugar itself has been evaluated with respect to rotations about its C_3-C_4 axis (see Fig. 1).

	A	T	G	C	Mean	Sugar
m	134	125	150	110	130	85
I	3.6×10^3	3.0×10^3	4.4×10^3	2.3×10^3	3.3×10^3	1.2×10^2
l	3.2	4.0	5.0	2.4	4.7	3.3
d_s	1.5	1.5	1.5	1.5	1.5	
d_b	2.0	2.0	2.0	2.0	2.0	

directly, and we will need to introduce various kinds of approximation.

We would like to stress that the choice of torsion angles as variables to describe our dynamics led to involved expressions, but our choices are very simple physically. We have in fact considered "angular harmonic" approximations (expansion up to first Fourier mode) i.e., potentials of the form $V(x)=[1-\cos(x)]$ for the torsion and helicoidal interactions, harmonic approximation for the base stacking interaction, and a harmonic potential depending on the intrapair distance for the pairing interaction.

It should also be stressed that our approximations are coherent with those considered in the literature when dealing with uniform models of the DNA chain, and in particular when dealing with (extensions of) the Yakushevich model. Thus when comparing the characteristic of our model with those of these other models, we are really focusing on the differences arising from considering separately the backbone unit and the base within each nucleotide.

It would of course be possible to consider more realistic expressions for the potentials; but we believe that at the present stage this would rather obscure the relevant point here, i.e., the discussion of how such "composite" models can retain the remarkable good features of the Y model and at the same time overcome some of the difficulties encountered by this.

V. PHYSICAL VALUES OF PARAMETERS

We should still assign concrete values to the parameters—both geometrical ones and coupling constants—appearing in our Lagrangian (4.1) and in the equation of motion (A1) when the model is applied to DNA.

A. Kinematical parameters

Let us start by discussing kinematical parameters; in these we include the geometrical parameters as well as the mass m and the moment of inertia I.

The masses can be readily evaluated by considering the chemical structure of the bases. They can be calculated just by knowing masses of the atoms and their multiplicity in the different bases. As for the geometrical parameters like R, a, r, and d_h (and the moment of inertia I), quite surprisingly different authors seem to provide different values for these. Rather than assuming the values given by one or another author, we have preferred to estimate the parameters using the available information about the DNA structure. The position of atoms within the bases (which of course determine R, a, r, and d_h, and hence I) and geometrical descriptions of DNA are widely available to the scientific community in the form of PDB files [47]. We will use this information (which we accessed at [48,49]) to estimate directly all static parameters in play on the basis of the atomic positions.

The geometrical parameters which are relevant for our discussion are the longitudinal width of bases l_b and of the sugar l_s, the distances of the bases from the relative sugars d_s, and the distance of a base from the relative dual base d_b. We give our estimates for the masses, moments of inertia, and the parameters l, d_s, and d_b for the different bases and their mean values in Table I. From those data and using the equations $R=l_s$, $r=\hat{d}_s+\hat{l}_b/2$, $d_h=\hat{l}_b+\hat{d}_s$, and $a=l_s+\hat{l}_b+\hat{d}_s+\hat{d}_b/2$ (hats denote mean values), one obtains the average values for the geometrical parameters appearing in our Lagrangian, given in Table II.

B. Coupling constants

The determination of the four coupling constants appearing in our model is more problematic, due partly to the difficulties in making experiments to test single coupling constants, and partly to the complexity of the system itself.

1. Pairing

The coupling constant K_p, which appears in the pairing potential (4.16) can be easily determined by considering the

TABLE II. Numerical values of the geometrical parameters characterizing our model.

R (Å)	r (Å)	d_h (Å)	a (Å)
3.3	3.8	6.2	10.5

typical energy of hydrogen bonds. The pairing interaction involves two (in the A-T case) or three (in the G-C case) electrostatic hydrogen bonds. The pairing potential can be modeled with a Morse function

$$V_p(x) = D(e^{-bd(x,x_0)} - 1)^2 = \frac{1}{2}(2Db^2)(\rho - \rho_0)^2 + O(\rho^3), \tag{5.1}$$

where D is the potential depth, ρ the distance from the equilibrium position ρ_0, and b a parameter that defines the width of the well. Although throughout this paper we use the harmonic potential (4.16) to model the pairing interaction, the use of the Morse function seems more appropriate for evaluating the parameter K_p. The point is that the pairing coupling constant is physically determined by the behavior of the pairing potential away from its minimum. Using the harmonic approximation (4.16) for estimate K_p would result in a completely unphysical value for the parameter.

Different estimates of the parameters appearing in the potential (5.1) are present in the literature. The estimates

$$D_{AT} = 0.030 \text{ eV}, \quad D_{GC} = 0.045 \text{ eV},$$

$$b_{AT} = 1.9 \text{ Å}^{-1}, \quad b_{GC} = 2.5 \text{ Å}^{-1}$$

are given in [51] and used in [52]. The values

$$D = 0.040 \text{ eV}, \quad b = 4.45 \text{ Å}^{-1}$$

are given in [53] and used in [17,53,54]. Finally, the estimates

$$D_{AT} = 0.050 \text{ eV}, \quad D_{GC} = 0.075 \text{ eV}, \quad b_{AT} = b_{GC} = 4 \text{ Å}^{-1}$$

are given in [55] and used in [55,56]. The values of coupling constants corresponding to these different values for the parameters appearing in the Morse potential range across a whole order of magnitude:

$$3.5 \text{ N/m} \leqslant K_p := 2b^2 D \leqslant 38 \text{ N/m}. \tag{5.2}$$

In our numerical investigations we will use a value of K_p near the lower bound given in Eq. (5.2); that is, we adopt the value $K_p = 4$ N/m, leading to an optical frequency of $\omega_0 = \sqrt{2K_p/m} = 36 \text{ cm}^{-1}$, so to be in agreement with [57].

2. Stacking

The determination of the torsion and stacking coupling constants is more involved and rests on a smaller amount of experimental data. The main information is the total torsional rigidity of the DNA chain $C = S\delta$, where $\delta = 3.4$ Å is the base-pair spacing and S is the torsional rigidity. It is known [58,59] that

$$10^{-28} \text{ J m} \leqslant C \leqslant 4 \times 10^{-28} \text{ J m}. \tag{5.3}$$

This information is used, e.g., in [1,60], whose estimate is based on the evaluation of the free energy of superhelical winding; this fixes the range for the total torsional energy to be

$$180 \text{ kJ/mol} \leqslant S \leqslant 720 \text{ kJ/mol}. \tag{5.4}$$

On the other hand, data about base flipping in DNA sequences indicate lower values of total free energy, of about 80 kJ/mol [37]. In this paper we will use for evaluating stacking and torsional coupling constants the highest of the two lower bound values, namely that coming from torsional rigidity results. Lower values for the torsion and stacking coupling constants will leave our results qualitatively unchanged, in particular, the system will remain well inside the stability region for the existence of solitons.

In our composite model the total torsional energy of the DNA chain has to be considered as the sum of two parts, the base stacking energy and the torsional energy of the sugar-phosphate backbone. In order to extract the stacking coupling constant we use the further information that $\pi - \pi$ stacking bonds amount at the most to 50 kJ/mol [61]. Assuming a quadratic stacking potential, as we do, and a width of the potential well of about 2 Å we obtain the estimate $K_s = 68$ N/m. The phonon speed induced by this is $c_1 = \delta\sqrt{K_s/m} \simeq 6$ km/s, see Eq. (6.10); this is rather close to the the estimate of 1.8 km/s $\leqslant c_1 \leqslant$ 3.5 km/s given in [26].

As we shall see in detail in Sec. IX, choosing smaller values for K_s would have nontrivial consequences since solitons with small topological numbers become unstable in the discrete setting when the ratios K_s/K_p and K_t/K_p get small enough (see Sec. IX). In particular, this value for K_s—together with the K_t below—is barely enough to allow the existence of solitons, as discussed later on in this paper.

3. Torsion and helicoidal couplings

After extracting the stacking component, our estimate for the torsional coupling constant K_t is in the range

$$130 \text{ kJ/mol} \leqslant K_t \leqslant 670 \text{ kJ/mol}. \tag{5.5}$$

Assuming (see below) that $K_h \simeq K_t/25$, so that $c_4 = \sqrt{2K_t/I_s}$ [see Eqs. (6.9) and (6.10)], all of these values for K_t induce phonon speeds slightly higher with respect to the estimates cited above, between 5 and 11 km/s. For our numerical investigations, to keep the phonon speed as low as possible, we will set $K_t = 130$ kJ/mol.

Finally, for the helicoidal coupling constant, following [62], we assume that K_t and K_h differ by about a factor of 25, so that $K_h = 5$ kJ/mol.

4. Discussion

It is interesting to point out how the geometry of the model nicely fits with the estimates of the binding energies so to induce optical frequencies and phonon speeds of the right order of magnitude (see also the discussion in Sec. VI). This is not the case in simpler models, where in order to get the right phonon speed within a simple Y model one is obliged to assume for K_t the unphysical value $K_t = 6000$ kJ/mol [26].

Our estimates, and hence our choices for the values of the coupling constants appearing in our model, are summarized in Table III. We will use these values of the physical parameters of DNA in the next sections, when discussing both the linear approximation and the dispersion relations as well as the full nonlinear regime and the solitonic solutions.

TABLE III. Values of the coupling constants for our DNA model.

K_t (kJ/mol)	K_s (N/m)	K_p (N/m)	K_h (kJ/mol)
130	68	3.5	5

VI. SMALL AMPLITUDE EXCITATIONS AND DISPERSION RELATIONS

In this section we will investigate the dynamical behavior of our model for small excitations in the linear regime. We will enforce the Yakushevich condition $R+d_h=a$ in order to keep the calculations and their results as simple as possible (see also [45]).

Linearizing the equation of motion (A1) around the equilibrium configuration

$$\varphi_i^{(a)} = \theta_i^{(a)} = \dot{\varphi}_i^{(a)} = \dot{\theta}_i^{(a)} = 0, \tag{6.1}$$

we get with standard algebra,

$$\begin{aligned} &mr^2\ddot{\varphi}_i^{(a)} + m(rR+r^2)\ddot{\theta}_i^{(a)} \\ &\quad = K_s[(rR+r^2)(\theta_{i+1}^{(a)} - 2\theta_i^{(a)} + \theta_{i-1}^{(a)}) + r^2(\varphi_{i+1}^{(a)} - 2\varphi_i^{(a)} \\ &\qquad + \varphi_{i-1}^{(a)})] - K_p[(a-R)^2(\varphi_i^{(a)} + \varphi_i^{(\hat{a})}) \\ &\qquad + a(a-R)(\theta_i^{(a)} + \theta_i^{(\hat{a})})]; \end{aligned}$$

$$\begin{aligned} &m(rR+r^2)\ddot{\varphi}_i^{(a)} + [I + m(R+r)^2]\ddot{\theta}_i^{(a)} = K_t[\theta_{i+1}^{(a)} - 2\theta_i^{(a)} + \theta_{i-1}^{(a)}] \\ &\quad + K_s(r+R)[(R+r)(\theta_{i+1}^{(a)} - 2\theta_i^{(a)} + \theta_{i-1}^{(a)}) + r(\varphi_{i+1}^{(a)} - 2\varphi_i^{(a)} \\ &\quad + \varphi_{i-1}^{(a)})] - K_p[(a^2 - aR)(\varphi_i^{(a)} + \varphi_i^{(\hat{a})}) + a^2(\theta_i^{(a)} + \theta_i^{(\hat{a})})] \\ &\quad + K_h(\theta_{i+5}^{(\hat{a})} - 2\theta_i^{(a)} + \theta_{i-5}^{(\hat{a})}). \end{aligned} \tag{6.2}$$

We are mainly interested in the dispersion relations for the propagating waves, which are solution of the system (6.2). To derive them it is convenient to introduce variables $\varphi^{(\pm)}$ and $\theta^{(\pm)}$ defined as

$$\varphi_i^{\pm} = \frac{1}{2}(\varphi_i^{(1)} \pm \varphi_i^{(2)}), \quad \theta_i^{\pm} = \frac{1}{2}(\theta_i^{(1)} \pm \theta_i^{(2)}). \tag{6.3}$$

Let us now Fourier transform our variables, i.e., set

$$\varphi_n^{\pm}(t) = F_{k\omega}^{\pm}\exp[i(k\delta n + \omega t)]; \quad \theta_n^{\pm}(t) = G_{k\omega}^{\pm}\exp[i(k\delta n + \omega t)]. \tag{6.4}$$

Here, k is the spatial wavenumber, ω is the wave frequency, and δ is a parameter with dimension of length and set equal to the interpair distance (δ=3.4 Å), introduced so that k has dimension $[L]^{-1}$ and the physical wavelength is $\lambda=2\pi/k$. In this way, we should only consider $k\in[-\pi/\delta,\pi/\delta]$.

Using Eqs. (6.3) and (6.4) into (6.2), we get a set of linear equations for $(F_{k\omega}^{\pm}, G_{k\omega}^{\pm})$; each set of coefficients with indices (k,ω) decouples from other wavenumber and frequency coefficients, i.e., we have a set of four-dimensional systems depending on the two continuous parameters k and ω. This is better rewritten in vector notation as

$$M\zeta_{k\omega} = 0, \tag{6.5}$$

where $\zeta_{k\omega}$ is the vector of components

$$\zeta_{k\omega} = (F_{k\omega}^{+}, F_{k\omega}^{-}, G_{k\omega}^{+}, G_{k\omega}^{-}) \tag{6.6}$$

and M is a four by four matrix which we omit to write explicitly.

In order to simplify the calculations we will set to zero the radius of the disk modeling the base, i.e., $d_h=r$. As in our model the disk describing the base cannot rotate around its axis, this assumption does not modify the physical outcome of the calculations.

The condition for the existence of a solution to Eq. (6.5) is the vanishing of the determinant of M. By explicit computation one finds that the equation $\|M\|=0$ has four solutions, given by

$$\begin{aligned} \omega_1^2 &= 4(K_s/m)\sin^2(k\delta/2), \\ \omega_2^2 &= 4(K_t/I)\sin^2(k\delta/2) + 2(K_h/I)[1+\cos(5k\delta)], \\ \omega_3^2 &= 2(K_p/m) + 4(K_s/m)\sin^2(k\delta/2), \\ \omega_4^2 &= 4(K_t/I)\sin^2(k\delta/2) + 4(K_h/I)\sin^2(5k\delta/2). \end{aligned} \tag{6.7}$$

Equations (6.7) provide the dispersion relations for our model.

Physically, the four dispersion relations correspond to the four oscillation modes of the system in the linear regime. The relation involving ω_1 describes relative oscillations of the two bases in the chain with respect to the neighboring bases. As $\omega_1(k)\to 0$ for $k\to 0$ there is no threshold for the generation of these phonon mode excitations.

The relations involving ω_2 and ω_4 are associated with torsional oscillations of the backbone. In case of ω_2 there is a threshold for the generation of the excitation originating in the helicoidal interaction, whereas the second torsional mode ω_4 has no threshold and is thus also of acoustical type. The dispersion relation involving ω_3 describes relative oscillations of two bases in a pair. The threshold for the generation of the excitation is now determined by the pairing interaction.

The dispersion relations (6.7) for values of the physical parameters given in Tables I and III are plotted in Fig. 3; there we plot $\omega/(2\pi c)$, where c is the speed of light (we use the, in the literature widespread, convention of measuring frequencies in $2\pi c$ units) versus $k\Delta/2$.

The four dispersion relations take a simple form if we consider excitations with wavelength λ much bigger than the intrapair distance, i.e., $\lambda \gg \delta$; this corresponds to the $\delta\to 0$ limit. We have then

$$\omega_\alpha^2 - c_\alpha^2 k^2 = q_\alpha^2, \tag{6.8}$$

where c_α and q_α ($\alpha=1\cdots4$) are, respectively, the velocity of propagation (in the limit $k\gg q_\alpha$) and the excitation threshold. They are given by

$$\begin{aligned} c_1 &= \delta\sqrt{K_s/m}, \quad q_1 = 0; \\ c_2 &= \delta\sqrt{(K_t - 25K_h)/I}, \quad q_2 = 2\sqrt{K_h/I}; \end{aligned}$$

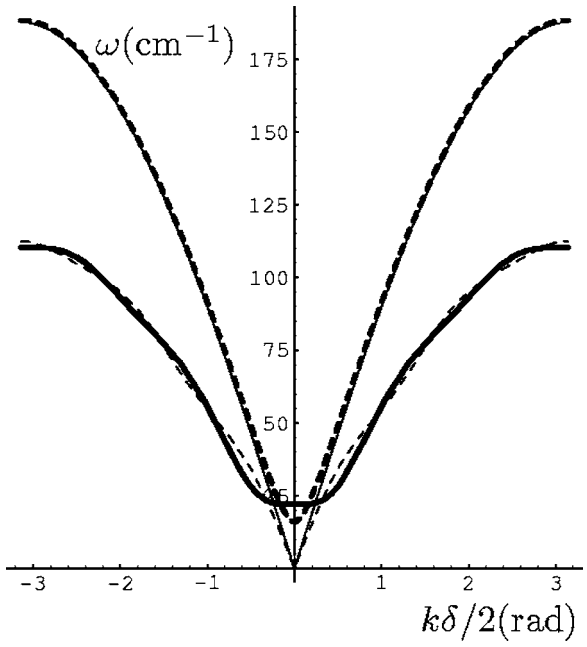

FIG. 3. Graph of the dispersion relations (6.7) in the first Brillouin zone. We plot $\omega_\alpha/(2\pi c)$ (c is the speed of light) as a function of $k\Delta/2$. The ω_1, ω_2, ω_3, and ω_4 are represented, respectively, by the thin continuous, thick continuous, thick dashed, and thin dashed line. Units are cm^{-1} in the vertical axis and radiants in the horizontal axis.

$$c_3 = \delta\sqrt{K_s/m}, \quad q_3 = \sqrt{2K_p/m};$$

$$c_4 = \delta\sqrt{(K_t + 25K_h)/I}, \quad q_4 = 0. \tag{6.9}$$

Using the values of the parameters given in Tables I and III we have

$$c_1 = 6.1 \text{ km/s}, \quad q_1 = 0;$$

$$c_2 = 0 \text{ km/s}, \quad q_2 = 22 \text{ cm}^{-1};$$

$$c_3 = 6.1 \text{ km/s}, \quad q_3 = 36 \text{ cm}^{-1};$$

$$c_4 = 5.1 \text{ km/s}, \quad q_4 = 0, \tag{6.10}$$

where $c_2=0$ comes from the fact that we are taking $K_t \simeq 25K_h$ (see Table III). This of course just means that c_2 is at least an order of magnitude smaller than the other c_i—and therefore negligible. Speeds can be converted to base per seconds by dividing each c_i by $\delta=3.4$ Å; excitation thresholds can be converted in inverse of seconds by multiplying each q_i by $2\pi c$, where c is the speed of light.

VII. NONLINEAR DYNAMICS AND TRAVELING WAVES

After studying the small amplitude dynamics of our model, we should now investigate the fully nonlinear dynamics. We are in particular interested in soliton solutions, and on a physical basis they should have—if the model has any relation with real DNA—a size of about 20 base pairs. This also means that such solutions vary smoothly on the length scale of the discrete chain, and we can pass to the continuum approximation. On the other hand, such a smooth variance assumption is not justified on the length scales (five base pairs) involved in the helicoidal interaction, and one should introduce nonlocal operators in order to take into account helicoidal interactions in the continuum approximation [25].

Luckily, numerical experiments show that—at least in the case of the original Yakushevich model—soliton solutions are very little affected by the presence or otherwise of the helicoidal terms (as could also be expected by their intrinsical smallness, in a context where they cannot play a qualitative role as for small amplitude dynamics) [25]. Thus we will from now on simply drop the helicoidal terms, i.e., set $K_h=0$.

A. Continuum approximation and field equations

The continuum description of the discrete model we are considering requires one to introduce fields $\Phi^{(a)}(z,t), \Theta^{(a)}\times(z,t)$ such that

$$\Phi^{(a)}(n\delta,t) \approx \varphi_n^{(a)}, \quad \Theta^{(a)}(n\delta,t) \approx \theta_n^{(a)}. \tag{7.1}$$

The continuum approximation we wish to consider is the one where we take

$$\Phi^{(a)}(x \pm \delta,t) \approx \Phi^{(a)}(x,t) \pm \delta\Phi_x^{(a)}(x,t) + (1/2)\delta^2\Phi_{xx}^{(a)}(x,t),$$

$$\Theta^{(a)}(x \pm \delta,t) \approx \Theta^{(a)}(x,t) \pm \delta\Theta_x^{(a)}(x,t) + (1/2)\delta^2\Theta_{xx}^{(a)}(x,t). \tag{7.2}$$

Inserting Eq. (7.2), and taking $K_h=0$, into the Euler-Lagrange equations (A1), we obtain a set of nonlinear coupled partial differential equations (PDEs) for $\Phi^{(a)}(x,t)$ and $\Theta^{(a)}(x,t)$, depending on the parameter δ. Coherently with Eq. (7.2), we expand these equations to second order in δ and drop higher order terms.

The equations we obtain in this way are symmetric in the chain exchange. We will be able to decompose their solutions into a symmetric and an antisymmetric part under the same exchange. In view of the considerable complication of the system, it is convenient to deal directly with the equations for these symmetric and antisymmetric parts and to enforce the Y contact approximation $R+d_h=a$.

The full equations in the symmetric case, i.e., for

$$\Theta^{(1)}(x,t) = \Theta^{(2)}(x,t) = \Theta(x,t), \quad \Phi^{(1)}(x,t) = \Phi^{(2)}(x,t) = \Phi(x,t) \tag{7.3}$$

and in the antisymmetric case

$$\Theta^{(1)}(x,t) = -\Theta^{(2)}(x,t) = \Theta(x,t), \tag{7.4}$$

$$\Phi^{(1)}(x,t) = -\Phi^{(2)}(x,t) = \Phi(x,t)$$

are still quite complex and are not reported here [they are given in Appendix, see Eqs. (A2) and (A3), respectively]. We will not consider the cases of mixed symmetry.

B. Soliton equations

When studying DNA models, one is specially interested in traveling wave solutions, i.e., solutions depending only on $z := x - vt$ with fixed speed v:

$$\Phi^{(a)}(x,t) = \varphi^{(a)}(x - vt) := \varphi^{(a)}(z), \tag{7.5}$$

$$\Theta^{(a)}(x,t) = \theta^{(a)}(x - vt) := \theta^{(a)}(z).$$

If we insert the ansatz (7.5) into Eqs. (A2) and (A3), we get a set of four coupled second order ordinary differential equations (ODEs); defining

$$\mu := (mv^2 - K_s\delta^2), \quad J := (Iv^2 - K_t\delta^2), \tag{7.6}$$

we obtain in the completely symmetric case (A2)

$$\begin{aligned}
&\mu r^2\varphi'' + \mu r(r + R\cos\varphi)\theta'' \\
&\quad = -2aK_p(a - R)\sin(\varphi + \theta) + K_s\delta^2 Rr\sin(\varphi)(\theta')^2 \\
&\qquad - R\sin(\varphi)[-2K_p(a - R) + mrv^2(\theta')^2]; \\
&\mu r(r + R\cos\varphi)\varphi'' + [J + \mu(R^2 + r^2 + 2Rr\cos\varphi)]\theta'' \\
&\quad = -2aK_p[R\sin\theta + (a - R)\sin(\varphi + \theta)] \\
&\qquad + \mu Rr\sin(\varphi)[(\varphi')^2 + 2\varphi'\theta'].
\end{aligned} \tag{7.7}$$

In the completely antisymmetric case (A3), we get instead

$$\begin{aligned}
&\mu r^2\varphi'' + \mu r(r + R\cos\varphi)\theta'' \\
&\quad = -2K_p(a - R)[a - R\cos\theta - (a - R)\cos(\varphi + \theta)] \\
&\qquad \times\sin(\varphi + \theta) - \mu Rr(\sin\varphi)(\theta')^2; \\
&\mu r(r + R\cos\varphi)\varphi'' + [J + \mu(R^2 + r^2 + 2Rr\cos\varphi)]\theta'' \\
&\quad = -K_p[2aR\sin\theta - R^2\sin(2\theta) + (a - R)\{2a\sin(\varphi + \theta) \\
&\qquad - (a - R)\sin[2(\varphi + \theta)] - 2R\sin(\varphi + 2\theta)\}] \\
&\qquad + \mu rR(\sin\varphi)[(\varphi')^2 + 2\varphi'\theta'].
\end{aligned} \tag{7.8}$$

The previous equations appear too involved to be studied analytically at least in the general case. Numerical results are discussed in Sec. IX below. Some understanding at the analytical level can be gained by considering a particular case of the full equations (7.7) and (7.8), when the system reduces essentially to the Y case. Section VIII is devoted to this.

C. Boundary conditions

We have so far just discussed the field equations (A2) and (A3) and their reductions; however, these PDEs make sense only once we specify the function space to which their solutions are required to belong. The natural physical condition is that of *finite energy*; we now briefly discuss what it means in terms of our equations and the boundary conditions it imposes on their solutions.

The field equations (A2) and (A3) are Euler-Lagrange equations for the Lagrangian obtained as a continuum limit of Eq. (4.1). In the present case, the finite energy condition corresponds to requiring that for large $|z|$ the kinetic energy vanishes and the configuration corresponds to points of minimum for the potential energy. The condition on kinetic energy yields

$$\Phi_t(\pm\infty,t) = 0, \quad \Theta_t(\pm\infty,t) = 0, \tag{7.9}$$

where of course $\Phi_t(\pm\infty,t)$ stands for $\lim_{z\to\pm\infty}\Phi_t(z,t)$, and so for Θ_t.

As for the condition involving potentials, by the explicit expression of these, see above, this means (with the same shorthand notation as above)

$$\begin{aligned}
&\Phi(\pm\infty,t) = 0, \quad \Theta(\pm\infty,t) = 2n_\pm\pi, \\
&\Phi_z(\pm\infty,t) = 0, \quad \Theta_z(\pm\infty,t) = 0.
\end{aligned} \tag{7.10}$$

Let us now consider the reduction to traveling waves, i.e., Eqs. (7.7) and (7.8). In this framework, conditions (7.9) and (7.10) imply we have to require the limit behavior described by

$$\begin{aligned}
&\varphi(\pm\infty) = 0, \quad \theta(\pm\infty) = 2n_\pm\pi, \\
&\varphi'(\pm\infty) = 0, \quad \theta'(\pm\infty) = 0,
\end{aligned} \tag{7.11}$$

for the functions $\varphi(\xi)$, $\theta(\xi)$. The solutions satisfying Eq. (7.11) can be classified by the winding numbers $n := n_+ - n_-$.

We would like to stress that Eqs. (7.7) and (7.8) can also be seen as describing the motion (in the fictitious time ξ) of point masses of unit mass, whose position has coordinates $\theta(\xi), \varphi(\xi)$, in an effective potential. Such a motion can satisfy the boundary conditions (7.11) only if $(\varphi,\theta) = (0, 2\pi k)$ is a point of maximum for the effective potential. This would provide the condition $\mu < 0$ and hence a maximal speed for soliton propagation (as also happens for the standard Y model); we will not discuss this point here, as it is no variation with the standard Y case, and the condition $\mu < 0$ is satisfied with the values of parameters obtained and discussed in Sec. V.

A similar discussion also applies to the full equations, i.e., those in which we have not selected any symmetry of the solutions; in this case we have two winding numbers (n_1, n_2), which we can associate to $(\theta^{(1)}, \theta^{(2)})$. When describing the solutions in terms of the symmetric and antisymmetric combinations $\theta^\pm = (1/2)(\theta^{(1)} \pm \theta^{(2)})$, we will have

$$\theta^+(\pm\infty) = 2p_\pm\pi, \quad \theta^-(\pm\infty) = 2q_\pm\pi, \tag{7.12}$$

whereas $p_\pm, q_\pm$ may assume both integers or half-integers values, owing to the 1/2 factor in the definition of $\theta^\pm$. Correspondingly, in these coordinates we will use the notation (p,q), with $p = p_+ - p_-$, $q = q_+ - q_-$, to indicate the soliton. Notice that whereas the winding numbers n_1, n_2 are integers, p, q may also assume half-integers values.

VIII. COMPARISON WITH THE YAKUSHEVICH MODEL

The geometry of the standard Y model [24] can be recovered as a limiting case of our model. As we considered here physical assumptions which correspond to those by Y in her geometry, a direct comparison of the results of our model with those of the standard Y model is obtained in this limit.

The standard Y model can be obtained as a limiting case of our composite model in two conceptually different ways.

(1) A first possibility, which we call *parametric* (or *geometric*), is to choose the geometrical parameters of the model so that its geometry actually reduces to that of the standard Y model.

(2) A second possibility, which we call *dynamical* is to force the dynamics of our model by setting $\varphi^a=0$, i.e., by freezing the nontopological angles and constraining them to be zero; equivalently, by setting the limit angle $\varphi_0=0$.

Let us briefly discuss these in some more detail. The parametric way consists in setting to zero the radius of the disks modeling the bases, and at the same time pushing it on the disk representing the backbone unit on the DNA chain. In this way the base corresponds to a point on the circle bounding the disk representing the backbone unit. Note that this would cause a change in the interbase equilibrium distance, unless we at the same time also change the radius of the disk representing the backbone unit.

This limiting procedure corresponds—recalling we also want to recover the Y approximation of zero interbase distance—to the following choice of the parameters:

$$m = K_s = d_h = r = 0, \quad a = R. \tag{8.1}$$

Note that once the base has been pushed on the disk, its mass is part of the disk's mass—and hence contributes to its moment of inertia—and we can thus just take $m=0$. Similarly, as the bases have lost their identity and are enclosed in the disk modeling the whole nucleotide, the effective stacking interaction has to be physically identified with the torsional interaction of the disk now modeling the entire nucleotide. For this reason in our equations we will take $K_s=0$ and $K_t \to \tilde{K}_s$. Use of Eqs. (8.1) into the equations of motion (A1) yields

$$I\ddot{\theta}_i^{(a)} = \tilde{K}_s \sin(\theta_{i-1}^{(a)} - \theta_i^{(a)}) + \tilde{K}_s \sin(\theta_{i+1}^{(a)} - \theta_i^{(a)}) + K_p R^2 \sin(\theta_i^{(a)} - \theta_i^{(\hat{a})}) + K_h(\theta_{i+5}^{(\hat{a})} - 2\theta_i^{(a)} + \theta_{i-5}^{(\hat{a})}). \tag{8.2}$$

The previous equations represent the equations of motions for the standard Y model.

Some care has to be used when the values of the parameters given by Eq. (8.1) correspond to singular points of the equations. This is, for instance, the case of the dispersion relations ω_1,ω_3 in Eqs. (6.7), which are singular for $m=0$. The dispersion relations for the Y model can be easily found by linearizing the system (8.2). One finds two dispersion relations; one is given by ω_2 of the composite model, see Eqs. (6.7); the other is

$$\omega^2 = 2R^2\frac{K_p}{I} + \frac{4K_s}{I}\sin^2\left(\frac{k\delta}{2}\right) + \frac{4K_h}{I}\sin^2\left(\frac{5k\delta}{2}\right). \tag{8.3}$$

Let us also discuss the dynamical reduction. To obtain the Y model dynamically from our model, we set $\Phi=0$ into the continuum equations (A2) and (A3). We also enforce the Y condition $R+d_h=a$ and work in the zero radius approximation for the disk modeling the base, i.e., set $r=d_h$.

In the fully symmetric case we get from Eqs. (A2)

$$m\Theta_{tt} = -2K_p \sin(\Theta) + \delta^2 K_s \Theta_{xx};$$

$$\left(\frac{I}{(R+r)^2} + m\right)\Theta_{tt} = -2K_p \sin\Theta + \delta^2\left[\frac{K_t}{(r+R)^2} + K_s\right]\Theta_{xx}. \tag{8.4}$$

Compatibility of the previous two equations requires that

$$I\Theta_{tt} = \delta^2 K_t \Theta_{xx}. \tag{8.5}$$

In the case of traveling wave solutions $\Theta(x,t)=\theta(x-vt)$ the constraint (8.5) reads

$$v^2 = \frac{\delta^2}{I}K_t. \tag{8.6}$$

We take from now on the positive determination of velocity for ease of discussion. Using Eqs. (7.5), (7.6), and (8.6), Eqs. (8.4) yield the traveling wave equation,

$$\theta'' = -2(K_p/\mu_0)\sin\theta, \tag{8.7}$$

where

$$\mu_0 = (mK_t - IK_s)\frac{\delta^2}{I}. \tag{8.8}$$

With the usual boundary conditions $\theta'(\pm\infty)=0$, $\theta(\infty)=2\pi$, $\theta(-\infty)=0$, Eq. (8.7) has a solution for $\mu_0<0$, given precisely by the (1, 0) Yakushevich soliton

$$\theta = 4\arctan[e^{\kappa z}], \quad \kappa = \sqrt{2K_p|\mu_0|}. \tag{8.9}$$

We have thus recovered for the topological angles—imposing the vanishing of nontopological angles as an external constraint—the Y solitons.

The condition for the existence of the soliton, $\mu_0<0$, implies that the physical parameters of our model must satisfy the condition

$$\frac{K_t}{I} < \frac{K_s}{m}. \tag{8.10}$$

With the parameter values given in Tables I and III, we have

$$\frac{mK_t}{IK_s} \simeq 0.3 < 1; \tag{8.11}$$

hence Eq. (8.10) is satisfied and we are in the region of existence of the soliton.

It should be stressed that in the standard Y model the traveling waves speed is essentially a free parameter, provided the speed is lower than a limiting speed [62,63]. Here, by recovering the standard Y model as a limiting case of the composite model we had a selection of the soliton speed, see Eq. (8.6). This makes sense physically, as it coincides with the speed of long waves determined by the dispersion relations (6.9).

IX. NUMERICAL ANALYSIS OF SOLITON EQUATIONS AND SOLITON SOLUTIONS

Even after the several simplifying assumptions we made for our DNA model, the complete equations of motions given by Eqs. (A2) and (A3), respectively, for symmetric and antisymmetric configurations, are too complex to be solved analytically; the same applies to the reduced equations (7.7) and (7.8) describing soliton solutions. We will thus look for solutions, and, in particular, for the soliton solutions we are interested in, numerically.

In order to determine the profile of the soliton solutions we will analyze the stationary case, with zero speed and kinetic energy, and apply the "conjugate gradients" algorithm (see, e.g., [64,65]) to evaluate numerically the minima of our Hamiltonian.

This approach also allows a direct comparison with the results obtained for the standard Yakushevich model, and shown in [26], where authors proceed in the same way and by means of the same numerical algorithm. In this way, once again, we emphasize the differences which are due purely to the different geometry of our "composite" model.

With the same motivation, we have also checked our numerical routines by applying them to the standard Y model; in doing this we have also considered with some care—and fully confirmed—certain nontrivial effects mentioned in [26].

A. Solitons in the composite Y model

We will consider the case when the intrapair distance at the equilibrium is zero, i.e., we will set $a=r+d_h$ (contact approximation). Notice that we are not considering the zero-radius approximation for the bases, so that in general $r \neq d_h$.

The Hamiltonian of the system can be easily derived from the Lagrangian (4.1) and is given by

$$H = T_B + T_b + V_t + V_s + V_p + V_h + V_w. \tag{9.1}$$

We use the shorthand notation

$$\psi_i = \theta_i^+, \quad \chi = \theta_i^-, \quad \xi_i = \varphi_i^+, \quad \eta_i = \varphi_i^-;$$

$$\Delta_i \psi = \psi_{i+1} - \psi_i, \quad \mathrm{S}_i \psi = \psi_{i+1} + \psi_i;$$

and similarly for the other variables; we also write

$$\alpha = R/r, \quad \beta = R/d_h;$$

with the values given in Table I, it results $\alpha=0.92$, $\beta=0.53$. The explicit expressions for the different terms of the Hamiltonian are easily obtained, and are reported for the sake of completeness in the Appendix, see Eq. (A4).

Note that we have inserted in the Hamiltonian the confining potential V_w in order to implement dynamically the constraint (3.1) for the nontopological angles $\varphi^{(a)}$. Adding this term in the potential is also instrumental in stabilizing the numerical minimizations.

The Hamiltonian (9.1) reduces to that of the Yakushevich model setting $\xi=\eta=0$ (and disregarding the helicoidal term); in this case V_t and V_s differ just by a multiplicative function. See the Appendix for details.

TABLE IV. Values of the typical energies characterizing the different interactions in the Hamiltonian of Eq. (A4).

E_t (kJ/mol)	E_s (kJ/mol)	E_p (kJ/mol)	E_h (kJ/mol)	E_w (kJ/mol)
2.6×10^2	2.9×10^3	4×10^2	10	4×10^{-1}

The typical energies involved in the different interactions are given by the coefficients in Eq. (A4), $E_t=2K_t$, $E_s=\frac{1}{2}K_s r^2$, $E_p=\frac{1}{2}K_p d_h^2$, $E_h=K_h$, and $E_w=K_w$; these represent, respectively, the typical torsional, stacking, pairing, helicoidal, and confining energies. Using the values of the physical parameters given in Tables I and III, and choosing E_w in order to keep the confining energy at least a full order of magnitude smaller than any other one, we get for the typical interaction energies the values given in Table IV.

In order to work with dimensionless quantities, throughout this section we will measure energies in terms of $E_p=(1/2)K_p d_h^2=4.0\times10^2$ kJ/mol. Using the values of the kinematical parameters given in Table II and those of the dynamical parameters given by Table III, the dimensionless coupling constants turn out to be

$$g_t = E_t/E_p = 0.65, \quad g_s = E_s/E_p = 7.2, \quad g_p = 1,$$

$$g_h = E_h/E_p = 0.026, \quad g_w = E_w/E_p = 0.001. \tag{9.2}$$

Note that Eq. (A5) implies that, in the limit $\xi=\eta=0$, the Yakushevich couplings (K,g) and our coupling constants are related by

$$K = 2(1+\beta)^2 g_p, \quad g = 2g_t + 4(1+\alpha)^2 g_s; \tag{9.3}$$

this also yields

$$\frac{g}{K} = \frac{g_t + 2(1+\alpha)^2 g_s}{(1+\beta)^2 g_p} \simeq \frac{g_t + 7.4 g_s}{2.3 g_p} \simeq 23. \tag{9.4}$$

We obtain an approximate profile of a soliton, subject to the boundary conditions (7.11), by minimizing numerically the Hamiltonian through the "conjugate-gradient" algorithm, in particular, through its implementations in the GSL [65] and in the Numerical Recipes [64].

To enforce a particular topological type for the soliton under study we fix the angles at the extremes of the chain using the boundary conditions (7.12): $\psi_{-\infty}=\chi_{-\infty}=0$ and $\psi_{+\infty}=2\pi p$, $\chi_{+\infty}=2\pi q$, while the nontopological angles are requested to be identically zero at the extremes. As a "starting point" for the algorithm (see above) we use the natural choice [26]

$$\psi_i = \pi p[1 + \tanh(\beta(2i - N))],$$

$$\chi_i = \pi q[1 + \tanh(\beta(2i - N))],$$

$$\xi_i = \eta_i = 0, \tag{9.5}$$

where β is a parameter used to adjust the profile of the initial configuration (the starting point) and N is the number of sites on the chain. The number N is of course much smaller than

in real DNA (usually $N=4000$ in our simulations) but large enough to ensure that ψ and χ are constant at the beginning and the end of the chain within the numerical precision of our computations.

There is a threshold for the coupling constants that must be passed for the solitons to be stable. We have observed that these instabilities strongly depend on the lattice size, and even on using an even or odd number of sites. In Fig. 4 we show the region of instability for solitons in the (g_t, g_s) plane when we fix the values of the other coupling constants to be $g_h=0.026$, $g_p=1$, and $g_w=0.001$.

We always reach the same minimum—within 10^{-5} in the energy and 10^{-2} in the angle—while β varies across almost two orders of magnitude, provided that $\beta \geqslant 4$ to avoid falling on the step solution.

In Fig. 5 we plot the $(p,q)=(0,1)$ soliton of our model, corresponding to topological winding numbers $(n_1,n_2)=(1,-1)$ soliton of our model, with the physical values of the normalized coupling constants given by Eq. (9.2) and compare them with those obtained for the Yakushevich model. The profiles of the topological angles change very little from the corresponding profiles of the Yakushevich solitons.

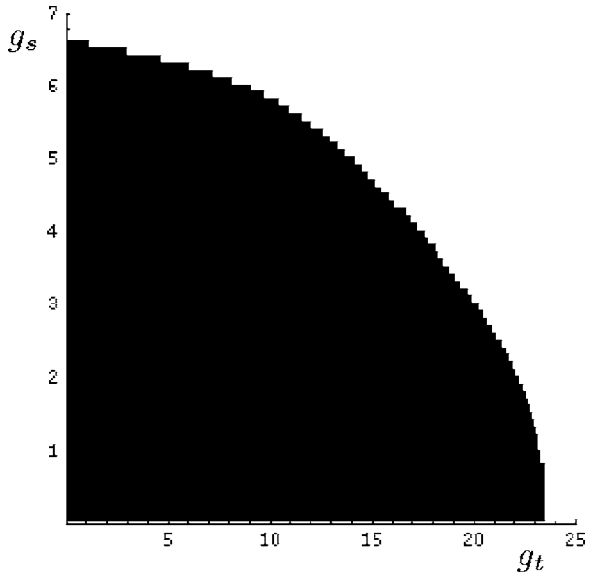

FIG. 4. Region of instability (black region) for the discrete solitons of topological type (0, 1) in the (g_t, g_s) plane.

B. Dependence on the parameters

We have also investigated the deformation of soliton profiles when adjusting selected parameters of our Hamiltonian. First, in order to see how the shape of the soliton changes upon increasing the strength of the torsional/stacking interactions, in Fig. 6 we compare the profiles of case $(p,q)=(1,0)$, corresponding to the soliton with $(n_1,n_2)=(1,1)$,

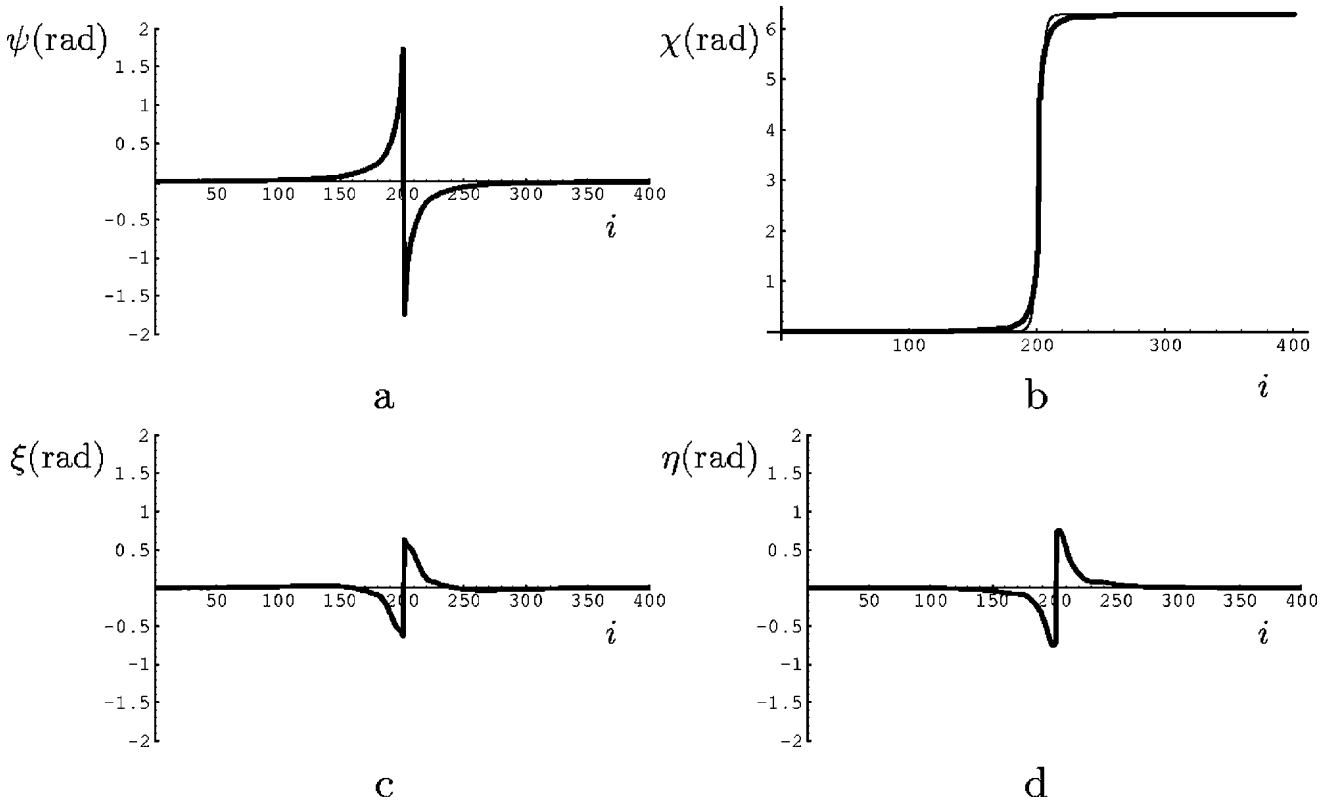

FIG. 5. Stationary solitonic solutions of our model with energy $E=80.06E_p$ (thick line) with $(p,q)=(0,1)$, corresponding to topological winding numbers $(n_1,n_2)=(1,-1)$, compared with the solitonic solutions of the Yakushevich model of energy $E=75.56E_p$ (thin line). Upper left (a): the angle ψ; upper right (b): the angle χ; lower left (c): the angle ξ; and lower right (d): the angle η. The thin line segments visible in (b) show the small difference between the profile of the solitons of our model and of the Yakushevich model.

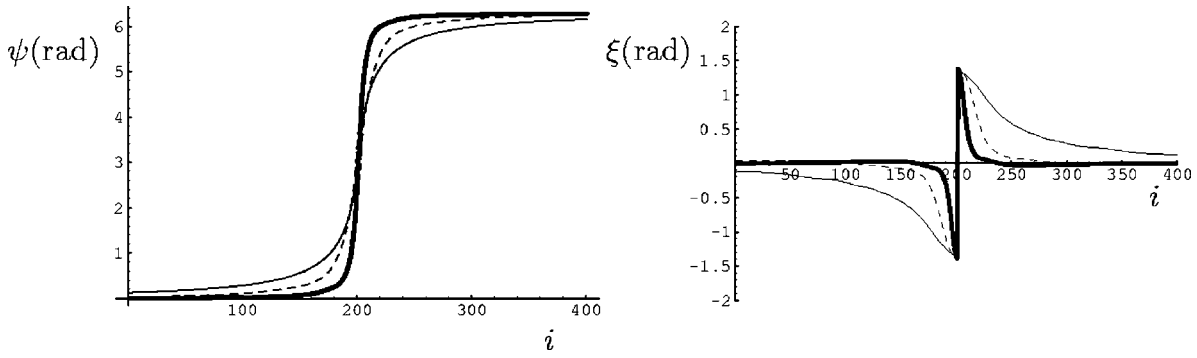

FIG. 6. Stationary solitonic solutions of our model with $(p,q)=(1,0)$, corresponding to topological winding numbers $(n_1,n_2)=(1,1)$, for different values of the normalized couplings. The angle ψ is depicted on the left whereas ξ is depicted on the right. The soliton relative to the physical coupling constants with energy $E=189.9E_p$ (thick line) is shown together with those relative to the coupling constants $g_t=0$, $g_s=46$ with energy $E=492.4E_p$ (thin dashed line) and $g_t=345$, $g_s=0$ (thin line, $E=388.5E_p$) to show how the profile would change at the increasing of the coupling constants in the two extreme cases of negligible torsional or stacking interactions.

with profiles corresponding to $g/K\simeq 150$ [see Eq. (9.4)], i.e., the coupling constant used in [26].

As it is not completely clear how to separate the interaction strength between torsional and stacking interactions (for our choice of physical constants in Sec. V), we have used about the smallest reasonable value for K_t. We present the profiles corresponding to the two extreme possibilities: the one in which we put all the strength in the backbone torsional interaction ($g_t=345$, $g_s=0$), and the one in which we put all of it in the bases stacking ($g_t=0$, $g_s=46$). The effect is the widening of both the soliton and the nontopological profiles by roughly a factor of 4 in the first case and of a factor of 2 in the second case.

In Fig. 7 we compare the profiles of case $(p,q)=(1/2,1/2)$, corresponding to the soliton with $(n_1,n_2)=(1,0)$, with those obtained by using the correct distance function for V_p, namely by replacing $g_p\rho^2$ with $g_p(\rho-d_0/d_h)^2$ (where $d_0\simeq 2$ Å is the equilibrium distance between two bases in a pair [66]), and by varying the helicoidal interaction term. No relevant changes are detected in the first case: relative differences in energies and angles are of the order of 10^{-2} in energy and 10^{-1} in the angles; even increasing the base-pairs distances by two orders of magnitude these results do not modify the situation.

As for the helicoidal term, we get variations of the same order of magnitude as above if we simply turn it off. If we

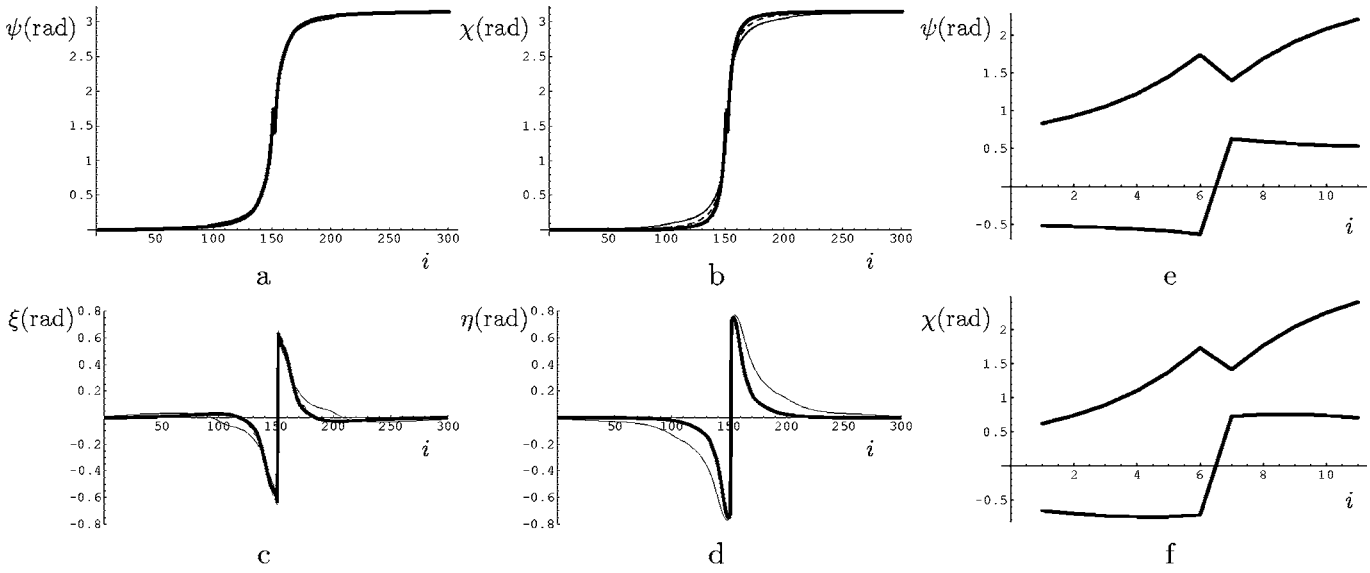

FIG. 7. Comparison of stationary solitonic solutions of our model for $(p,q)=(1/2,1/2)$, corresponding to topological winding numbers $(n_1,n_2)=(1,0)$, with those obtained using a modified pairing potential V_p. Upper left (a): the angle ψ; upper right (b): the angle χ; lower left (c): the angle ξ; and lower right (d): the angle η. The thick line represents a soliton of our model with $E=80.06$. The thin dashed line gives the profile for the same soliton with energy $E=74.41E_p$ and with the "correct" pairing potential $V_p=g_p(\rho-d_0/d_h)^2$. The latter solitonic solution has been derived taking $d_0=3.2d_h$, namely an order of magnitude bigger than its physical value, to enhance the profile differences (an almost identical profile is obtained if we suppress the helicoidal term from the Hamiltonian). The thin continuous line ($E=102.9E_p$) is the profile we get by increasing the helicoidal term to $g_h=1$. Finally, we show a detail of the step present at the center of the soliton in the angles ψ (e) and χ (f) together with the respective nontopological angles; as expected, the sugar angles slightly jump, exactly at the moment when the bases hit the sugars and bounce back.

instead increase the coupling constant by one order of magnitude ($g_h=0.26$), then we get energy and angles changes of the order of 10^{-1} and by increasing it to $g_h=1$ we arrive at changes of the order of 10^0 in both the angles and the energy.

Raising g_h up to $g_h=2$ leads to the disappearance of the soliton; it seems reasonable to argue that this is due to such an interaction favoring a sharper transition between limit behaviors, so that the discreteness effect discussed in the previous section arises.

C. Discussion

The numerical analysis we have performed shows the existence of solitonic solutions of our composite DNA model. The profiles of the topological solitons—in particular, the part relating to the topological degree of freedom—of our model are both qualitatively and quantitatively very similar to those of the Y model. This means that the most relevant (for DNA transcription) and characterizing feature of the nonlinear DNA dynamics present in the Y model is preserved by considering geometrically more complex and hence more realistic DNA models.

Moreover, the topological soliton profiles of our model seem to change very little when either the physical parameters change in a reasonable range or also the form of the potential modeling the pairing interaction is modified to a more realistic form. In particular, the form of the topological solitons are very little sensitive to the interchange of torsional and stacking coupling constant.

This feature adds other reasons why the Y model, although based on a strong simplification of the DNA geometry, works quite well in describing solitonic excitations. The Y model, indeed, does not distinguish between torsional and stacking interaction; but, as we have shown, this distinction is not relevant—at least as long as one is only interested in the existence and form of the soliton solutions.

The "compositeness" of our model becomes relevant—and rather crucial—when it comes on the one hand to allowing the existence of solitons *together* with requiring a physically realistic choice of the physical parameters characterizing the DNA, and on the other hand to have also predictions fitting experimental observations for what concerns quantities related to small amplitude dynamics, such as transverse phonons speed. In other words, the somewhat more detailed description of DNA dynamics provided by our model allows it to be effective—with the same parameters—across regimes, and provide meaningful quantities in both the linear and the fully nonlinear regime. The solitonic solutions of the composite model share also another feature with those of the Y model, namely the presence of a numerical instability.

We expect that the model considered here is the simplest DNA model describing rotational degrees of freedom which, with physically realistic values of the coupling constants and other parameters, allows for the existence of topological solitons and at the same time is also compatible with observed values of bound energies and phonon speeds in DNA.

X. SUMMARY AND CONCLUSIONS

Let us, in the end, summarize our discussion and the results of our work, and state the conclusions which can be drawn from it.

A. Summary and results

Following the work by Englander *et al.* [1], different authors have considered simple models of the DNA double chain—focusing on rotational degrees of freedom—able to support dynamical and topological solitons [4], supposedly related to the transcription bubbles present in real DNA and playing a key role in the transcription process.

These models usually consider a single (rotational) degree of freedom per nucleotide [4], albeit models with one rotational and one radial degree of freedom per nucleotide have also been considered [17–19,27,28] (as an extension of "purely radial" models [5,15], considered in the study of DNA denaturation).

A simple model which has been studied in depth is the so-called Y model [24]. This supports topological solitons (of sine-Gordon type) and provides correct orders of magnitude for several physically relevant quantities [25]; on the other hand, the soliton speed remains essentially a free parameter [62,63], and the speed of transverse phonons can be made to have a physical value only by assigning unphysical values to the coupling constants of the model [26].

Here we have considered an extension of the Y model, with two degrees of freedom—both rotational—per nucleotide; one of these is associated to rotations of the backbone unit (sugar-phosphate group) around the phosphodiester chain and is topological—i.e., can go around the S^1 circle—while the other is associated to rotations of the attached nitrogen base around the C_1 atom in the sugar ring, and due to sterical hindrances is nontopological, i.e., rotations are limited to a relatively small range around the equilibrium position. We denoted this as a "composite Y model."

Several parameters appear in the model; some of these are related to the geometry and the kinematics of the DNA molecule, while others are coupling constants entering in the potential used to model intramolecular interactions. We have assigned values to the first kind of parameters from available direct experimental observations, while for the second kind of parameters we used experimental data on the ionization energies of the concerned couplings and the form of the potentials appearing in the model. That is, these parameters were *not* chosen by fitting dynamical predictions of the model; see Sec. V for details.

We have first considered small amplitude dynamics (Sec. VI); this yields the dispersion relations and produced some prediction on the phonon speed and the optical frequency for the different branches. These prediction are a first success of the present model, in that it was shown in Sec. VI that one can obtain—with physical values for the parameters—the order of magnitude of the experimentally observed speed for transverse phonon excitations and the frequency threshold for the optical branch.

In particular, we get a value for the transverse phonon speed which is about three times the "correct" one. It should be considered, in looking at this value, that we modeled the intrapair interaction by a very simple and nonrealistic potential (with the aim of both keeping computations simple and allowing direct comparison with the standard Y model by making the same simplifying assumptions as there). As for comparison with the standard Y model, hence for an evalu-

ation of the advantages brought by considering a more articulated geometry of the nucleotide, it should be recalled that the numerical computations of Yakushevich, Savin, and Manevitch [26] (which we repeated, and fully confirmed) show that in order to obtain the experimentally observed speed for transverse phonon excitations in the framework of the standard Y model, one should take a coupling constant for the transverse intrapair interaction which is about 6000 times the physical one.

We then passed to consider the fully nonlinear regime, and in particular to look for solitoniclike traveling excitations. These should have smooth variations on the space scale of nucleotides, hence we passed to a continuum description and field equations; by using the chain exchange symmetry, we considered fully symmetric and antisymmetric reductions. By a traveling wave ansatz we reduced these to a system of two coupled second order ODEs for $\theta(z)$ and $\varphi(z)$, see Eqs. (7.7) and (7.8). Here θ is the topological angle, i.e., the variable associated to the topological field, and φ is the nontopological angle, i.e., the variable associated to the nontopological field.

The finite energy conditions (7.9) and (7.10) require that the solutions to this system of ODEs satisfy certain limit conditions [see Eq. (7.11)]. These in turn imply that solutions satisfying them can be classified according to two topological indices (winding numbers for the topological fields; in the symmetric or antisymmetric case, one index is enough to determine the other as well).

We have also shown that the standard Y model can be obtained from the composite Y model by a limiting procedure (Sec. VII); this also reduces the solitons of the composite model to solitons of the Y model. However, the limiting procedure requires that a certain condition is satisfied, see Eq. (8.5), and this in turn constrains the speed of solitonic excitations; see Eq. (8.6). Thus the requirement to obtain the standard Y solitons in a certain limit fixes the speed of solitons; the resulting speed is just the speed of long waves as determined by the dispersion relations.

Finally, in Sec. IX we conducted a careful numerical investigation of the simpler soliton solutions for the composite Y model. We preliminarily checked our numerical routines on the standard Y model and fully confirmed the results of Yakushevich, Savin, and Manevitch [26], also confirming certain instability phenomena they reported (furthermore, we observed these instabilities can also strongly depend on the lattice size, and even on using an even or odd number of sites). We considered the solitons for the composite Y model with the value of parameters descending from their physical meaning (i.e., with no parameter fitting), confirming their existence, properties, and stability. We also showed how the profile of the soliton component corresponding to the topological degree of freedom is extremely similar to the standard Y soliton with the same topological numbers. We considered next the stability of these soliton solutions upon varying the parameters of the model, and observed that as in the standard Y case there is a stability threshold. Thus the existence and stability of soliton solutions for physical values of the parameters is a nontrivial prediction.

B. Discussion and conclusions

The composite Y model considered here retains all the favorable features of the standard Y model. At the same time, its more articulated geometry allows at the same time—and with physical values of the coupling constants and other parameters entering in the model—to reproduce a relevant value of physical quantities related to the linear regime (such as speed of transverse phonon, which was a critical test for the standard Y model) and support stable soliton solutions.

Further, and at difference with the standard Y model, it provides a precise prediction for the soliton speed; this is quite reasonable physically, as it corresponds to the speed of long waves as obtained from the dispersion relations for the model. Thus our model passed some—in our opinion, significant—quantitative tests and provides precise predictions.

It should also be stressed that we used—both to simplify the mathematics and to have a direct comparison with the standard Y model—a very simple form for the intrapair coupling potential (and also resorted to the "contact approximation" to get simpler formulas, again as in the standard Y model treatment). It is quite conceivable that adopting a more realistic potential will provide better estimates of relevant physical quantities, in particular, for quantities related to the linear regime. However, experience recently gained with the standard Y model [44,45] suggests that the predictions related to the fully nonlinear regime are rather little sensitive to the detailed form of the potential and to adopting or otherwise the contact approximation; we are thus rather confident that future work with more realistic potentials will confirm the results obtained in the simple setting considered here.

Admittedly, the model studied here—as all models of DNA dynamics in the literature—disregards nonconservative effects in DNA dynamics; these are known to be relevant, as DNA is actually an overdamped system subject to random forces due to interactions with its fluid environment in the living cell. We believe, however, that an understanding of DNA dynamics *per se* should be reached before attempting to model also its complex interactions with the environment.

Finally, we would like to remark on a very relevant feature of our model. All the DNA models amenable to analytic treatment look at homogeneous DNA, albeit the genetic information lies precisely in the nonhomogeneous part of the DNA (i.e., the base sequence; bases have rather different physical and geometrical characteristics). Our discussion was no exception, and we considered identical bases with "average" geometrical and physical characteristics; but, the degrees of freedom we considered for each nucleotide are one concerned with the uniform part of the DNA molecule (the backbone units), the other with the nonhomogeneous part (the base sequence). Moreover, it turned out that—for what concerns soliton excitations—the most relevant role is played by the (topological) variables associated to the uniform part, which are directly at play in the topological solitons, while the (nontopological) variables associated to the nonuniform part are in a way just accompanying the soliton.

This suggests that, within the framework of composite models, the nonhomogeneous case can be studied as a (nonsingular) perturbation of the homogeneous case; needless to say, by this we mean an analytical—albeit approximated—study, and not just a numerical one. This represents a significant advance with respect to what is possible with simple models considered so far.

ACKNOWLEDGMENT

This work wassupported by the Italian MIUR (Ministero dell'Istruzione, Università e Ricerca) under the program COFIN2004, as part of the PRIN project "Mathematical Models for DNA Dynamics ($M^2 \times D^2$)."

APPENDIX: EXPLICIT EQUATIONS

In this appendix we collect some explicit equations that we have not provided in the main text due to their complex structure. The purpose of this is to enable the reader wishing to enter into the details of our study to see the detailed equations, without interrupting the main stream of our discussion by lengthy formulas, which are of little interest to the nonspecialized reader.

We start by providing the explicit form of the Euler-Lagrange equations corresponding to the Lagrangian (4.1). With our choices for the different terms of L, see Sec. IV, and writing $\hat{a}$ for the complementary chain of the chain a (that is, $\hat{1}=2$, $\hat{2}=1$), these read

$$
\begin{aligned}
&mr^2\ddot{\varphi}_i^{(a)} + mr[R\cos(\varphi_i^{(a)}) + r]\ddot{\theta}_i^{(a)} + mrR\sin(\varphi_i^{(a)})(\dot{\theta}_i^{(a)})^2 \\
&\quad = K_s r^2 \sin[\varphi_{i-1}^{(a)} - \varphi_i^{(a)} + \theta_{i-1}^{(a)} - \theta_i^{(a)}] - 2ad_hK_p\sin(\varphi_i^{(a)} + \theta_i^{(a)}) - K_srR\sin(\varphi_i^{(a)} - \theta_{i-1}^{(a)} + \theta_i^{(a)}) - K_srR\sin(\varphi_i^{(a)} + \theta_i^{(a)} - \theta_{i+1}^{(a)}) \\
&\qquad - K_s r^2\sin(\varphi_i^{(a)} - \varphi_{i+1}^{(a)} + \theta_i^{(a)} - \theta_{i+1}^{(a)}) + d_hK_pR\sin(\varphi_i^{(a)} + \theta_i^{(a)} - \theta_i^{(\hat{a})}) + d_h^2K_p\sin(\varphi_i^{(a)} - \varphi_i^{(\hat{a})} + \theta_i^{(a)} - \theta_i^{(\hat{a})}) \\
&\qquad + R(d_hK_p + 2K_sr)\sin[\varphi_i^{(a)}];
\end{aligned}
$$

$$
\begin{aligned}
&mrR\cos(\varphi_i^{(a)})(\ddot{\varphi}_i^{(a)} + 2\ddot{\theta}_i^{(a)}) + mr^2\ddot{\varphi}_i^{(a)} + I\ddot{\theta}_i^{(a)} + mr^2\ddot{\theta}_i^{(a)} + mR^2\ddot{\theta}_i^{(a)} - mrR\sin(\varphi_i^{(a)})\dot{\varphi}_i^{(a)}(\dot{\varphi}_i^{(a)} + 2\dot{\theta}_i^{(a)}) = (K_t + K_sR^2)\sin(\theta_{i-1}^{(a)} - \theta_i^{(a)}) \\
&\quad + K_srR\sin[\varphi_{i-1}^{(a)} - (\theta_i^{(a)} - \theta_{i-1}^{(a)})] - K_sr^2\sin[(\varphi_i^{(a)} - \varphi_{i-1}^{(a)}) + (\theta_i^{(a)} - \theta_{i-1}^{(a)})] - 2aK_pR\sin(\theta_i^{(a)}) - 2ad_hK_p\sin(\varphi_i^{(a)} + \theta_i^{(a)}) \\
&\quad - K_srR\sin[\varphi_i^{(a)} + (\theta_i^{(a)} - \theta_{i-1}^{(a)})] - K_srR\sin[\varphi_i^{(a)} - (\theta_{i+1}^{(a)} - \theta_i^{(a)})] + (K_t + K_sR^2)\sin(\theta_{i+1}^{(a)} - \theta_i^{(a)}) + K_sr^2\sin[(\varphi_{i+1}^{(a)} - \varphi_i^{(a)}) + (\theta_{i+1}^{(a)} \\
&\quad - \theta_i^{(a)})] + K_srR\sin[\varphi_{i+1}^{(a)} + (\theta_{i+1}^{(a)} - \theta_i^{(a)})] + K_pR^2\sin(\theta_i^{(a)} - \theta_i^{(\hat{a})}) + d_hK_pR\sin[\varphi_i^{(a)} + (\theta_i^{(a)} - \theta_i^{(\hat{a})})] + d_h^2K_p\sin[(\varphi_i^{(a)} - \varphi_i^{(\hat{a})}) + (\theta_i^{(a)} \\
&\quad - \theta_i^{(\hat{a})})] - d_hK_pR\sin[\varphi_i^{(\hat{a})} - (\theta_i^{(a)} - \theta_i^{(\hat{a})})] + K_h(\theta_{i+5}^{(\hat{a})} - 2\theta_i^{(a)} + \theta_{i-5}^{(\hat{a})}).
\end{aligned} \tag{A1}
$$

Note that here a, R, and d_h are considered as independent parameters, i.e., we have not enforced the Yakushevich condition $R+d_h=a$ (equivalently $\rho_0=0$).

In Sec. VII we considered the continuum approximation for our model and in particular for Eqs. (A1), but gave explicitly only the traveling wave reductions. Here we give the complete form of the continuous Euler-Lagrange equations.

In the symmetric case, i.e., for $\Theta^{(1)}(x,t)=\Theta^{(2)}(x,t)=\Theta(x,t)$ and $\Phi^{(1)}(x,t)=\Phi^{(2)}(x,t)=\Phi(x,t)$, the resulting equations are

$$
\begin{aligned}
&mr^2\Phi_{tt} + (mr^2 + mRr\cos\Phi)\Theta_{tt} \\
&\quad = -2a(a-R)K_p\sin(\Phi+\Theta) - R[2K_p(R-a) + mr\Theta_t^2]\sin\Phi + \delta^2K_sr[r(\Phi_{xx}+\Theta_{xx}) + R\Theta_{xx}\cos\Phi \\
&\qquad + R\Theta_x^2\sin\Phi];
\end{aligned}
$$

$$
\begin{aligned}
&(mr^2 + mRr\cos\Phi)\Phi_{tt} + [I + m(R^2 + r^2 + 2Rr\cos\Phi)]\Theta_{tt} \\
&\quad = -2aK_p[R\sin\Theta + (a-R)\sin(\Phi+\Theta)] + m\Phi_t \times Rr(\Phi_t + 2\Theta_t)\sin\Phi + \delta^2\{K_sr^2\Phi_{xx} \\
&\qquad + [K_t + K_s(R^2 + r^2)]\Theta_{xx} + K_sRr[(\Phi_{xx} + 2\Theta_{xx})\cos\Phi - \Phi_x(\Phi_x + 2\Theta_x)\sin\Phi]\}.
\end{aligned} \tag{A2}
$$

In the antisymmetric case $\Theta^{(1)}(x,t)=-\Theta^{(2)}(x,t)=\Theta(x,t)$ and $\Phi^{(1)}(x,t)=-\Phi^{(2)}(x,t)=\Phi(x,t)$, the resulting equations are

$$
\begin{aligned}
&mr^2\Phi_{tt} + (mr^2 + mRr\cos\Phi)\Theta_{tt} \\
&\quad = K_p(a-R)\{R\sin(\Phi+2\Theta) + (a-R)\sin[2(\Phi+\Theta)] - 2a\sin(\Phi+\Theta)\} + R[K_p(a-R) - mr\Theta_t^2]\sin\Phi \\
&\qquad + \delta^2K - sr[r(\Phi_{xx}+\Theta_{xx}) + R\cos(\Phi)\Theta_{xx} + R\sin(\Phi)\Theta_x^2];
\end{aligned}
$$

$$
\begin{aligned}
&(mr^2 + mRr\cos\Phi)\Phi_{tt} + [I + m(R^2 + r^2 + 2Rr\cos\Phi)]\Theta_{tt} \\
&\quad = K_p(-2aR\sin\Theta + R^2\sin(2\Theta) + (a-R)\{-2a \times \sin(\Phi+\Theta) + (a-R)\sin[2(\Phi+\Theta)] + 2R \\
&\qquad \times \sin(\Phi+2\Theta)\}) + m\Phi_t rR(\Phi_t + 2\Theta_t) \times \sin\Phi + \delta^2\{K_sr^2\Phi_{xx} + K_t\Theta_{xx} + K_s(R^2 + r^2)\Theta_{xx}
\end{aligned}
$$

$$+ K_s rR[(\Phi_{xx} + 2\Theta_{xx})\cos\Phi - \Phi_x(\Phi_x + 2\Theta_x)\sin\Phi]\}. \tag{A3}$$

We will not write the equations in the cases of mixed symmetry, i.e., for $\Theta^{(1)}(x,t)=\Theta^{(2)}(x,t)=\Theta(x,t)$, $\Phi^{(1)}(x,t)=-\Phi^{(2)}(x,t)=\Phi(x,t)$ and for $\Theta^{(1)}(x,t)=-\Theta^{(2)}(x,t)=\Theta(x,t)$, $\Phi^{(1)}(x,t)=\Phi^{(2)}(x,t)=\Phi(x,t)$.

In Sec. IX our numerical study was conducted within the Hamiltonian formalism. The Hamiltonian (9.1), with the notation introduced there, reads

$$T_B = \sum_i I_B(\Delta_i\psi^2 + \Delta_i\chi^2),$$

$$T_b = \sum_i I_b[\Delta_i\xi^2 + \Delta_i\eta^2 + \Delta_i\psi^2 + \Delta_i\chi^2 + 2\Delta_i\psi\Delta_i\xi + 2\Delta_i\chi\Delta_i\eta + \alpha^2(\Delta_i\psi^2 + \Delta_i\chi^2) + 2\alpha(\Delta_i\psi^2 + \Delta_i\chi^2 + \Delta_i\psi\Delta_i\xi + \Delta_i\chi\Delta_i\eta)\cos\xi_i\cos\eta_i + 2\alpha(2\Delta_i\psi\Delta_i\chi + \Delta_i\chi\Delta_i\xi + \Delta_i\psi\Delta_i\eta)\sin\xi_i\sin\eta_i],$$

$$V_t = 2K_t\sum_i[\cos\Delta_i\psi\cos\Delta_i\chi - 1],$$

$$V_s = \frac{1}{2}K_s r^2\sum_i 4\{1 + \alpha^2 - \alpha^2\cos(\Delta_i\psi)\cos(\Delta_i\chi) - \cos(\Delta_i\chi + \Delta_i\eta)\cos(\Delta_i\psi + \Delta_i\xi) + 2\alpha\cos[(S_i\xi - S_i\eta)/2]\sin[(\Delta_i\psi - \Delta_i\chi)/2]\sin[(\Delta_i\psi - \Delta_i\chi + \Delta_i\xi - \Delta_i\eta)/2] + 2\alpha\cos[(S_i\xi + S_i\eta)/2]\sin[(\Delta_i\psi + \Delta_i\chi)/2]\sin[(\Delta_i\psi + \Delta_i\chi + \Delta_i\xi + \Delta_i\eta)/2]\},$$

$$V_p = \frac{1}{2}K_p d_h^2\sum_i 4[(1+\beta)^2 + \cos^2(\chi_i + \eta_i) + 2\beta\cos\chi_i\cos\xi_i\cos(\chi_i + \eta_i) + \beta^2\cos^2\chi_i - 2\beta(1+\beta)\cos\psi_i\cos\chi_i - 2(1+\beta)\cos(\psi_i + \xi_i)\cos(\chi_i + \eta_i)],$$

$$V_h = K_h\sum_i[2 - \cos(\psi_{i+5} - \chi_i) - \cos(\chi_{i+5} - \psi_i)],$$

$$V_w = K_w\sum_i[\tanh(\xi_i + \eta_i) + \tanh(\xi_i - \eta_i)]. \tag{A4}$$

As already remarked in Sec. IX, the Hamiltonian (A4) reduces to that of the Yakushevich model setting $\xi=\eta=0$ (and disregarding the helicoidal term); with this we get

$$T_B = I_B\sum_i(\Delta_i\psi^2 + \Delta_i\chi^2),$$

$$T_b = I_b(1+\alpha^2)\sum_i[\Delta_i\psi^2 + \Delta_i\chi^2],$$

$$V_t = 2K_t\sum_i[\cos\Delta_i\psi\cos\Delta_i\chi - 1],$$

$$V_s = \frac{1}{2}K_s r^2\sum_i 4(1+\alpha)^2[1 - \cos\Delta_i\psi\cos\Delta_i\chi],$$

$$V_p = \frac{1}{2}K_p d_h^2\sum_i 4(1+\beta)^2[1 - 2\cos\psi_i\cos\chi_i + \cos^2\chi_i], \tag{A5}$$

[1] S. W. Englander, N. R. Kallenbach, A. J. Heeger, J. A. Krumhansl, and A. Litwin, Proc. Natl. Acad. Sci. U.S.A. **77**, 7222 (1980).

[2] A. S. Davydov, *Solitons in Molecular Systems* (Kluwer, Dordrecht, 1981).

[3] It should be stressed that when we speak of "mechanical models" we exclude consideration of the all-important interactions between DNA and its environment. The latter includes at least the fluid in which DNA is immersed, and interaction with this leads to energy exchanges; one should thus include in the equations describing DNA dynamics both dissipation terms and random terms due to interaction with molecules in the fluid. We will work here at a purely mechanical level, i.e., do not consider at present these effects. Moreover, it should be mentioned that even forgetting dissipative and Brownian motion effects, one could consider interaction with the solvent by including effective terms in the intrapair potential V_p (see below), as done, e.g., in [52]; these take into account the effect of counterions neutralizing the phosphate charge (these counterions have a relevant impact on the DNA persistence length). It has been recently shown that in the context of the Peyrard-Bishop model this leads to a sharpening of certain transitions [67]. As for modeling the interaction between DNA and environment, see [68].

[4] L. V. Yakushevich, *Nonlinear Physics of DNA*, 2nd ed. (Wiley, Chichester, 2004).

[5] M. Peyrard, Nonlinearity **17**, R1 (2004).

[6] *Nonlinear Excitations in Biomolecules*, Proceedings of a workshop held in Les Houches, 1994, edited by M. Peyrard (Springer, Berlin and Les Editions de Physique, Paris, 1995).

[7] C. Calladine and H. Drew, *Understanding DNA* (Academic Press, London, 1992); C. Calladine, H. Drew, B. Luisi, and A. Travers, *Understanding DNA*, 3rd ed. (Academic Press, London, 2004).

[8] M. D. Frank-Kamenetskii, Phys. Rep. **288**, 13 (1997).

[9] W. Saenger, *Principles of Nucleic Acid Structure* (Springer, Berlin, 1984).

[10] *Nonlinear Phenomena in Biology*, Proceedings of the Pushchino Conference, 1998, edited by M. Peyrard [J. Biol. Phys. **24**, 97 (1999)].

[11] R. Lavery, A. Lebrun, J. F. Allemand, D. Bensimon, and V. Croquette, J. Sci. Comput. **14**, R383 (2002).

[12] F. Ritort, J. Sci. Comput. **18**, R531 (2006).

[13] T. R. Strick, M. N. Dessinges, G. Charvin, N. H. Dekker, J. F.

Allemand, D. Bensimon, and V. Croquette, Rep. Prog. Phys. **66**, 1 (2003).
[14] These were initiated about 15 years ago [69], but their range and precision has dramatically increased in recent years; the formation of bubbles in a double-stranded DNA has been observed in [70].
[15] M. Peyrard and A. R. Bishop, Phys. Rev. Lett. **62**, 2755 (1989).
[16] Th. Dauxois, Phys. Lett. A **159**, 390 (1991).
[17] M. Barbi, S. Cocco, and M. Peyrard, Phys. Lett. A **253**, 358 (1999); **253**, 161 (1999).
[18] M. Barbi, S. Cocco, M. Peyrard, and S. Ruffo, J. Biol. Phys. **24**, 97 (1999).
[19] S. Cocco and R. Monasson, Phys. Rev. Lett. **83**, 5178 (1999).
[20] M. Barbi, S. Lepri, M. Peyrard, and N. Theodorakopoulos, Phys. Rev. E **68**, 061909 (2003).
[21] S. Cuesta-Lopez, J. Errami, and M. Peyrard, J. Biol. Phys. **31**, 273 (2005).
[22] S. Cuenda and A. Sanchez, Chaos **16**, 023123 (2006).
[23] N. Theodorakopoulos, M. Peyrard, and R. S. MacKay, Phys. Rev. Lett. **93**, 258101 (2004).
[24] L. V. Yakushevich, Phys. Lett. A **136**, 413 (1989).
[25] G. Gaeta, C. Reiss, M. Peyrard, and Th. Dauxois, Riv. Nuovo Cimento **17**, 1 (1994).
[26] L. V. Yakushevich, A. V. Savin, and L. I. Manevitch, Phys. Rev. E **66**, 016614 (2002).
[27] L. V. Yakushevich, Stud. Biophys. **140**, 163 (1991).
[28] M. Joyeux and S. Buyukdagli, Phys. Rev. E **72**, 051902 (2005); S. Buyukdagli, M. Sanrey, and M. Joyeux, Chem. Phys. Lett. **419**, 434 (2006).
[29] It is appropriate, in this context, to mention earlier models proposed by Fedyanin, Gochev, and Lisy [71], Muto *et al.* [72], Prohofsky [73], Takeno and Homma [74], van Zandt [75], Yomosa [76], and Zhang [60].
[30] This is indeed an "open bubble" of about 20 bases, to which RNA polymerase (RNAP) binds in order to read the base sequence and produce the RNA messenger; the RNAP travels along the DNA double chain, and so does the unwound region.
[31] G. Gaeta, Phys. Lett. A **143**, 227 (1990).
[32] G. Gaeta, Phys. Lett. A **168**, 383 (1992).
[33] J. A. Gonzalez and M. Martin-Landrove, Phys. Lett. A **191**, 409 (1994).
[34] L. V. Yakushevich, Physica D **79**, 77 (1994).
[35] Needless to say, if such a more detailed modeling would produce results very near to those of the simple Y model, this should be seen as a confirmation that the latter correctly captures the relevant features of DNA torsional dynamics and hence justify *a posteriori* feature (a) of the Y model.
[36] It is usual, for ease of language, to refer to models in which helicoidal interactions are taken into account as "helicoidal," and to models in which they are overlooked as "planar." Needless to say, the geometry of the model is the same in both cases.
[37] N. K. Banavali and A. D. MacKerell, Jr., J. Mol. Biol. **319**, 141 (2002).
[38] This assumption (see also Sec. IX) is common to all the mathematical—as opposed to physicochemical—models of DNA, and as already remarked is necessary to be able to perform an analytical study of the model. We refer, e.g., to [4,5] for discussions about this point. Study of real sequences, i.e., with different characteristics for different bases, is possible numerically; see, e.g., [52,77].
[39] At the level of the numerical analysis the simplest way to implement this constraint is to use a confining potential, which reproduces approximately the form of a box. For this reason in Sec. IX we will add to the Hamiltonian of the system a confining potential $V_w = K \tan^4 \varphi^{(a)}$.
[40] A more realistic choice could have important consequences of qualitative—and not just quantitative—behavior of nonlinear excitations. This point is discussed in [78].
[41] The stacking interactions are of essentially electrostatic nature; thus it is reasonable in this context to see the bases as dipoles. If we have two identical dipoles made of charges $\pm\alpha$ a distance d apart, their separation vector being along the z direction, and force them to move in parallel planes orthogonal to the z axis and a distance L apart, then denoting with σ the distance of their projections in the (x,y) plane we have
$$V(\rho) = (1/2)\alpha[(d+L)^{-3} - 2L^{-3} + (d-L)^{-3}]\sigma^2 - (3/8)\alpha[(d+L)^{-5} - 2L^{-5} + (d-L)^{-5}]\sigma^4 + O(\sigma^6).$$
[42] The interaction does more properly depend on the degree of superposition of projections to bases on the plane orthogonal to the double helix axis (and moreover, depends on the details of charge distribution on each base), and in particular, quickly goes to zero once the bases assume different positions. Moreover, once the bases extrude from the double helix there are ionic interactions between the bases and the solvent which should be taken into account [52]. In this note, however, we will disregard these considerations—based also on [44]—and just consider harmonic stacking.
[43] As noted by Gonzalez and Martin-Landrove [33] in the context of the Yakushevich model, one should be careful in expanding a potential $V_p(\rho)$ in terms of the rotation angles φ and θ: indeed, unless $\rho_0 = 0$, i.e., $a = R + d_h$, one would get a zero quadratic term in such an expansion (see, however, [45] for what concerns solitons in this context).
[44] G. Gaeta, e-print q-bio/0604004, J. Nonlinear Math. Phys. (to be published).
[45] G. Gaeta, Phys. Rev. E **74**, 021921 (2006).
[46] In physical terms, this is not obvious by itself, as the filaments could have to wind around the double helix if the two connected backbone units are twisted by 2π with respect to each other; however, when this happens the filaments are actually broken and then built again thanks to quantum fluctuations.
[47] PDB repository, http://www.rcsb.org/pdb/
[48] H. R. Drew, R. M. Wing, T. Takano, C. Broka, S. Tanaka, K. Itakura, and R. E. Dickerson, Proc. Natl. Acad. Sci. U.S.A. **78**, 2179 (1981).
[49] PDB files at http://chemistry.gsu.edu/glacton/PDB/pdb.html
[50] http://chemistry.gsu.edu/glactone/
[51] Y. Z. Chen and E. W. Prohofsky, Phys. Rev. E **47**, 2100 (1992).
[52] F. Zhang and M. A. Collins, Phys. Rev. E **52**, 4217 (1995).
[53] Th. Dauxois, M. Peyrard, and A. R. Bishop, Phys. Rev. E **47**, 684 (1992).
[54] J. De Luca, E. Drigo Filho, A. Ponno, and J. R. Ruggiero, Phys. Rev. E **70**, 026213 (2004).
[55] A. Campa, Phys. Rev. E **63**, 021901 (2000).
[56] N. Komarova and A. Soffer, Bull. Math. Biol. **67**, 701 (2005).
[57] J. W. Powell, G. S. Edwards, L. Genzel, F. Kremer, A. Wittlin,

W. Kubasek, and W. Peticolas, Phys. Rev. A **35**, 3929 (1987).
[58] M. D. Barkley and B. H. Zimm, J. Chem. Phys. **70**, 2991 (1979).
[59] N. Bruant, D. Flatters, R. Lavery, and D. Genest, Biophys. J. **77**, 2366 (1999).
[60] Ch. T. Zhang, Phys. Rev. A **35**, 886 (1987); **40**, 2148 (1989).
[61] C. A. Hunter and J. K. M. Sanders, J. Am. Chem. Soc. **112**, 5525 (1990); R. Khairoutdinov, http://www.uaf.edu/chem/467Sp05/lecture4.pdf
[62] G. Gaeta, J. Biol. Phys. **24**, 81 (1999).
[63] G. Gaeta, Phys. Lett. A **190**, 301 (1994).
[64] Numerical Recipes, see http://www.library.cornell.edu/nr/bookfpdf/f10-6.pdf
[65] http://www.gnu.org/software/gsl/manual/gsl-ref_35.html#SEC474
[66] In order to avoid any confusion, we stress that here the "distance" between bases refers to the O-H distance in a N-H-O hydrogen bond; the total length of the bond is about 3 Å, and often one refers to this as the interbase distance. Here instead we consider the H atom—which lies at about 1 Å from the nearer atom in the H bond—as part of one of the bases and hence consider the distance of it from the other atom as the interbase distance.
[67] G. Weber, Europhys. Lett. **73**, 806 (2006).
[68] G. Lamm and A. Szabo, J. Chem. Phys. **85**, 7334 (1986).
[69] S. B. Smith, L. Finzi, and C. Bustamante, Science **258**, 1122 (1992).
[70] G. Altan-Bonnet, A. Libchaber, and O. Krichevsky, Phys. Rev. Lett. **90**, 138101 (2003).
[71] V. K. Fedyanin, I. Gochev, and V. Lisy, Stud. Biophys. **116**, 59 (1984); V. K. Fedyanin and V. Lisy, *ibid.* **116**, 65 (1984).
[72] V. Muto, J. Holding, P. L. Christiansen, and A. C. Scott, J. Biomol. Struct. Dyn. **5**, 873 (1988); V. Muto, P. S. Lomdahl, and P. L. Christiansen, Phys. Rev. A **42**, 7452 (1990).
[73] E. W. Prohofsky, Phys. Rev. A **38**, 1538 (1988).
[74] S. Takeno and S. Homma, Prog. Theor. Phys. **70**, 308 (1983); S. Homma and S. Takeno, *ibid.* **72**, 679 (1984).
[75] L. L. Van Zandt, Phys. Rev. A **40**, 6134 (1989).
[76] S. Yomosa, Phys. Rev. A **27**, 2120 (1983); Phys. Rev. A **30**, 474 (1984).
[77] M. Salerno, Phys. Rev. A **44**, 5292 (1991).
[78] G. Saccomandi and I. Sgura, J. R. Soc., Interface **3**, 655 (2006).